FRICTION FACTOR FOR GRAVEL-BED CHANNEL WITH HIGH BOULDER CONCENTRATION[a]

Discussion by Hossein Afzalimehr[2]

The discusser would like to comment on the paper from two viewpoints: first, the author's insight on the friction factor problem, and second, a realistic insight on the author's paper. The first viewpoint: It seems that the ASCE Task Force on Hydromechanics Committee (1963) has stated the final word on the progress in the flow resistance problem, which is that any progress in this subject depends on the concept of boundary layers. To justify this statement using the author's paper, the discusser applied some experimental results for small scale ($h/d_{50} > 4$) (Afzalimehr and Anctil 1999) and intermediate scale ($2 < h/d_{50} < 4$) (Afzalimehr and Anctil 2000) in which h is flow depth and d_{50} is characteristic diameter. First, it was considered that the condition ''flow is uniform on average'' is not realistic and at laboratory scale this condition can lead to considerable error for coarse-bed channels. Also, when concentration and h/d_{50} are constant, there is considerable variation in friction factor because of the bottom slope and discharge variation. Accordingly, when concentration is constant and discharge varies from 0.04 m^3/s to 0.076 m^3/s, the friction factor varies from 11.6 to 9.31 based on application of the boundary layers concept. Using uniform flow assumption, the friction factor varies from 0.88 to 1.66. So one can claim that it is not roughness geometry or concentration of coarse materials that affect the friction factor, it is the use of the unrealistic assumption that affects the friction factor. On the other hand, two cases were investigated for a given reference area. For the first case $d_{50} = 80$ mm, $Q = 0.054$ m^3/s, $h = 0.28$, and $S_0 = 0.007$; for the second case $d_{50} = 25.4$ mm, $Q = 0.054$ m^3/s, $h = 0.28$ m, and $S_0 = 0.007$, in which Q = flow discharge and S_0 is the bottom slope of the channel. It is evident that the concentration for the first case is less than the second case for a given reference area, but the friction factor for the first and second cases were obtained as 9.18 and 9.69, respectively. The difference was 5%. So it is realistic to ask where the effect of concentration is.

The second viewpoint: The discusser does not agree with the author's statement that ''the introduction of Froude number (F_r) into the flow resistance equation (14) is not useful. . . .'' To support the discusser's opinion, 140 gravel-bed rivers from different regions of the world were considered (Afzalimehr 1998) and were divided by four classes: $F_r < 0.3$, $0.3 < F_r < 0.6$, $0.6 < F_r < 0.9$ and $F_r > 0.9$. Accordingly, the effect of the first and second classes on the relationship of the logarithmic term with τ_{*c}/τ_{*c} is not remarkable with the coefficient of determination, $R^2 = 0.389$ for the first class and $R^2 = 0.32$ for the second class. On the other hand, for the third class $0.6 < F_r < 0.9$ there is considerable effect of the logarithmic term on τ_{*c}/τ_{*c}, in which τ_{*c} is the critical value of the Shields parameter, τ_*, with $R^2 = 0.614$. It was observed for this class that the larger τ_{*c}/τ_{*c}, the smaller the flow resistance. Finally, for the fourth class, the effect of the logarithmic term on the τ_{*c}/τ_{*c} is not clear with $R^2 = 0.20$. The reasons for this have been partly explained by Jarrett (1991) and are due to the difficulty in accurately measuring the flow structure as a result of very high velocity fluctuation and relatively small flow depth. In fact there is a great difference in turbulent structures between the low Froude number flow and high Froude number flows, which have a considerable effect on the shear velocity distribution that is a vital parameter for flow resistance estimation. Also, the application of τ_* as an independent variable on the right hand of (14) can make this equation implicit, because for estimation of C on the left hand, one needs to know S_0 and h as well as an estimate of τ_* on the right hand (14).

Finally, the objective of equations such as (14) is to improve the intercept of logarithmic equation in order to obtain the equilibrium between the left and right hand of (14). But there is considerable error in estimation C (friction factor), especially when one takes into account theoretical considerations like the boundary layer concept. So what can be obtained with any adjustment of intercept? An estimate of C on the left hand (14) or a realistic understanding of flow resistance problem?

APPENDIX. REFERENCES

Afzalimehr, H. (1998). ''Contribution to non-uniform open channel flows over gravel and cobble.'' PhD dissertation, Laval, University, Quebec, Canada.

Afzalimehr, H., and Anctil, F. (1999). ''Velocity distribution and shear velocity behavior of decelerating flows over a gravel bed.'' *Can. J. Civ. Engrg*., Ottawa, Aug.

ASCE Task Force on Hydromechanics Committee. (1963). ''Friction factors in open channels.'' *J. Hydr. Div*., ASCE, 89(2), 97–143.

Jarrett, R. D. (1991). ''Hydraulics of mountain rivers.'' *Channel flow resistance, centennial of Manning's formula*, B. C. Yen, ed., Water Resources Publications, Littleton, Colo., 287–298.

Closure by Vito Ferro[3]

The author thanks the discusser for his interest in this technical note and for providing the author further opportunity to clarify his results on the friction factor for gravel-bed channels.

In a gravel-bed river, according to Bathurst (1982) the flow has to be considered *uniform on average* because the roughness elements, varying in size and shape, being projecting or nonprojecting elements from the channel bed and being emerging or non-emerging from the flow, locally disrupt the river flow.

For the large-scale roughness, previous studies (Herbich and Shulits 1964; Judd and Peterson 1969; Bathurst 1978; Thompson and Campbell 1979; Bathurst et al. 1981) suggested that the flow resistance is mainly due to the *pattern* of the elements and their *arrangement* in the channel.

Two main processes of energy degradation must be considered in order to evaluate the flow resistance. The first of these two processes is the pattern (shape, size) and arrangement (spacing, orientation with respect to flow direction, and relative exposure of the elements from the channel bed) of the roughness elements on the channel boundary (*grain resistance*). The second process is linked to the energy degradation due to flow separation and macroscale eddies that occur for a change of channel alignment, of the cross-section shape, of slope, etc. (Bray 1987). Essentially the energy degradation is a jet and wake process: the flow accelerates to pass between the elements of the gravel bed and its energy degradation is associated with large-scale eddies.

The discusser compared the friction factor values for two experimental runs having the same discharge, water depth, and channel slope values and two values of the particle diameter

[a]July 1999, Vol. 125, No. 7, by Vito Ferro (Paper 15167).

[2]Asst. Prof., Dept. of Irrig., Isfahan Univ. of Technology, Isfahan, Iran 84156.

[3]Prof., PhD, Dipartimento di Ingegneria e Tecnologie Agro-Forestali, Sezione Idraulica, Facoltà di Agraria, Università di Palermo, Viale delle Scienze, 90128 Palermo, Italy. E-mail: vferro@unipa.it

d_{50} (80 and 25.4 mm). The two experimental runs gave friction factor values having a difference of 5%, and they concluded that the effect of the concentration can be neglected.

The discusser considered two bed arrangements only having a different characteristic diameter d_{50}, and give no information on the grain-size distribution of the bed particles. If the used gravel bed is not a mixture of two components (bed layer and boulders), then the bed particle grain-size distributions are not bimodal and each distribution differs from the other one only for a scale factor (different d_{50} value).

As an example, the grain-size distribution of each bed arrangement can be a lognormal law (see curve I and C of Fig. 2) having a different mean value of the bed particle diameter and the same standard deviation. Differences on the bed particle distributions restricted to the median diameter can explain little differences in the friction factor values.

For defining geometry of roughness, seven parameters can be used:

1. The *characteristic size* of the bed elements d_{xx}.
2. The *median size ratio* equal to the ratio between the median diameter of coarser particles and the median diameter of bed layer.
3. The *concentration* of boulders representing the weight of the coarser component in the mixture.
4. The *longitudinal distance* L_f of the elements, i.e., the distance between two elements measured along the flow direction. The knowledge of this distance with reference to the characteristic size allows one to establish if there is any interference among the eddies, having an horizontal axis, generated by the elements. In fact, if the distance between the elements of roughness is sufficient then the wake generated by each element is dissipated before meeting the following element (semi-smooth turbulent flow). As soon as the elements approach each other, the wake generated by each element does not extinguish before meeting the next one (hyperturbulent flow). Finally, if the elements are so close that between them an eddie is confined, then the flow motion takes place on a surface placed at the top level of the elements (quasi smooth flow) (Morris 1959).
5. The *transverse distance* L_t of the elements allows one to establish whether the eddies with vertical axis, generated by roughness elements, interfere.
6. The *arrangement* (regular or random) and the *orientation* of the elements with respect to flow direction.
7. The *shape* of the element (rounded cobbles, quarry rubble elements).

Baiamonte et al. (1995) carried out some experimental runs for evaluating the influence of the arrangement (regular and random) of the boulders on the flow resistance law. The three investigated regular bed arrangements were characterized by the same number of boulders N (equal concentration Γ) arranged on the ground layer, and the coarser elements were arranged on two rows with a relative distance L_f equal to 0, 12, and 24 cm.

For investigating the effect of the orientation, Baiamonte et al. (1995) carried out two other experimental runs using 20 coarser elements arranged on two rows perpendicular and parallel to the flow direction.

For $h/d_{50} < 5$, the measurements showed that the flow resistance relationship (h/d_{50}, $C/\sqrt{g}$) of the three regular arrangements, having different relative distance L_f, in the plane ($\log h/d_{50}$, $C/\sqrt{g}$) are represented by straight lines lower than the one corresponding to a random arrangement having the same boulder concentration.

For a small-scale roughness condition ($h/d_{50} > 5$), the influence of both the relative distance between two rows of coarser elements and the orientation of the elements respect to the flow direction of the flow resistance law become negligible; in other words, for $h/d_{50} > 5$ each bed arrangement is characterized only by the concentration of boulders.

For evaluating the influence of the element shape, Baiamonte et al. (1995) obtained two different bed arrangements using rounded river cobbles and quarry rubble elements having the same characteristic size. For the two investigated arrangements the following flow resistance relationships were obtained:

$$\frac{C}{\sqrt{g}} = 11.1 \log\left(\frac{h}{d_{50}}\right) + 3.68 \tag{17}$$

for rounded river cobbles, and

$$\frac{C}{\sqrt{g}} = 11.1 \log\left(\frac{h}{d_{50}}\right) + 3.12 \tag{18}$$

for quarry rubble elements.

The comparison between (17) and (18) shows that the two flow resistance laws are parallel in the plane $\log h/d_{50}$, $C\sqrt{g}$; therefore, for the investigated arrangements the influence of the element shape is independent of the depth/sediment ratio h/d_{50}.

At laboratory scale the uniform flow is easily obtainable using a slope flume, even if large-scale disturbance and eddies can be visualized for increasing values of the flow Froude number. Recently, laboratory observation of nonuniform open-channel flows and efforts for estimating flow resistance for nonuniform flow conditions were also carried out (Song and Graf 1984; Kirinoto and Graf 1995; Afzalimehr and Anctil 2000).

Eq. (16) established that the ratio τ/τ_{*cr} and the Froude number signify the same information in the flow resistance law; therefore, if the sediment mobility parameter is introduced into the flow resistance equation the further introduction of F is redundant information. In other words, the flow resistance law (6) can be improved introducing either the sediment mobility parameter or the Froude number.

The relationship between sediment mobility parameter and the Froude number is theoretically derived [(16)] in the paper. In any case, as it is known, the initial movement of the bed particles (critical condition) can be explained by critical velocity equations or critical shear stress equations. These two approaches, which might appear to be different, are not entirely different from each other (Graf 1984).

For a uniform flow having a uniform flow depth h, and cohesionless particles having a diameter d and a specific weight γ_s, using the critical velocity V_c approach, the condition of incipient movement is expressed by the following functional relationship (Neill 1967):

$$f(V_c^2, \mu, h, \rho, d, \gamma_s - \gamma) = 0 \tag{19}$$

in which f is a functional symbol; μ = water viscosity; and ρ = water density. According to the Π-theorem of dimensional analysis (Barenblatt 1987), the same functional relationship [(19)] can be expressed using only three dimensionless groups:

$$f(\Pi_1, \Pi_2, \Pi_3) = 0 \tag{20}$$

where Π_1, Π_2, Π_3, are dimensionless groups whose expression has to be determined. Choosing ρ, d, and $\gamma_s - \gamma$ as dimensional independent variables (i.e., as the measurement units of a particular reference system), Π_1 has the following expression:

$$\Pi_1 = \rho^{\alpha} d^{\beta} (\gamma_s - \gamma)^{\varepsilon} V_c^2 \tag{21}$$

where α, β, and ε are numerical constants. Substituting the measurement units of each variable, (21) gives

$$0 = kg^{\alpha}\ s^{2\alpha}\ m^{-4\alpha}\ m^{\beta}\ kg^{\varepsilon}\ m^{-3\varepsilon}\ m^{2}\ s^{-2} \tag{22}$$

The numerical values of the three constants, α, β, and ε are easily calculated solving the following system:

$$0 = \alpha + \varepsilon \tag{23a}$$

$$0 = 2\alpha - 2 \tag{23b}$$

$$0 = -4\alpha + \beta - 3\varepsilon + 2 \tag{23c}$$

The solution of the system ($\alpha = 1$, $\beta = \varepsilon = -1$) substituted into (21) gives the following expression of the dimensionless group Π_1:

$$\Pi_1 = \frac{\rho V_c^2}{(\gamma_s - \gamma)d} \tag{24}$$

In a similar way, the following expression of Π_2 and Π_3 can be deduced:

$$\Pi_2 = \frac{\mu}{\rho^{1/2}(\gamma_s - \gamma)^{1/2}d^{3/2}} \tag{25}$$

$$\Pi_3 = \frac{h}{d} \tag{26}$$

Taking into account that the ratio V_c/u^* depends on h/d, it results in

$$\frac{\Pi_1^{1/2}}{\Pi_2} = \frac{\rho^{1/2}V_c(\gamma_s - \gamma)^{1/2}\rho^{1/2}d^{3/2}}{(\gamma_s - \gamma)^{1/2}d^{1/2}\mu} = \frac{V_c d}{\upsilon} = \left(\frac{u^* d}{\upsilon}\right)\varphi\left(\frac{h}{d}\right) = R^*\varphi\left(\frac{h}{d}\right) \tag{27}$$

in which R^* is the shear Reynolds number and φ is a functional symbol. Π_1 can be rearranged as follows:

$$\Pi_1 = \frac{\rho V_c^2}{(\gamma_s - \gamma)d}\frac{gh}{gh} = \frac{h}{d}\frac{\gamma}{(\gamma_s - \gamma)}\frac{V_c^2}{gh} = \frac{h}{d}\frac{F^2}{\lambda} \tag{28}$$

in which $\lambda = (\gamma_s - \gamma)/\gamma$.

In conclusion, the incipient motion condition can be expressed using the following explicit functional relationship:

$$\frac{F}{\sqrt{\gamma}} = \varphi\left(R^*, \frac{h}{d}\right) \tag{29}$$

in which φ is a functional symbol.

Following the critical shear stress τ_c approach, the condition of incipient motion is expressed by the following functional relationship:

$$f(\tau_c, \mu, h, \rho, d, \gamma_s - \gamma) = 0 \tag{30}$$

and this functional relationship can be expressed as (20). Choosing ρ, d, and $\gamma_s - \gamma$, as dimensional independent variables, Π_1 has the following expression:

$$\Pi_1 = \rho^{\alpha}d^{\beta}(\gamma_s - \gamma)^{\varepsilon}\tau \tag{31}$$

where α, β, and ε are numerical constants. Substituting the measurement units of each variable, (31) gives

$$0 = kg^{\alpha}\ s^{2\alpha}\ m^{-4\alpha}\ m^{\beta}\ kg^{\varepsilon}\ m^{-3\varepsilon}\ kg\ m^{-2} \tag{32}$$

The numerical values of the three constants, α, β, and ε are easily calculated solving the following system:

$$0 = \alpha + \varepsilon + 1 \tag{33a}$$

$$0 = 2\alpha \tag{33b}$$

$$0 = -4\alpha + \beta - 3\varepsilon - 2 \tag{33c}$$

The solution of the system ($\alpha = 0$, $\beta = \varepsilon = -1$) substituted into (31) gives the following expression of the dimensionless group Π_1:

$$\Pi_1 = \frac{\tau}{(\gamma_s - \gamma)d} \tag{34}$$

while the expressions of Π_2 and Π_3 are the same of (25) and (26). Eqs. (34) and (25) give

$$\frac{\Pi_1^{1/2}}{\Pi_2} = \frac{\tau^{1/2}(\gamma_s - \gamma)^{1/2}\rho^{1/2}d^{3/2}}{(\gamma_s - \gamma)^{1/2}d^{1/2}\mu}\frac{\rho^{1/2}}{\rho^{1/2}} = \frac{u^* d}{\upsilon} = R^* \tag{35}$$

Therefore, the incipient motion condition can be expressed using the following explicit functional relationship:

$$\frac{\tau}{(\gamma_s - \gamma)d} = \varphi\left(R^*, \frac{h}{d}\right) \tag{36}$$

Comparing (36) and (29) shows that the Shields number and the ratio $F/\sqrt{\lambda}$ signify the same information. In other words, taking into account that the experimental runs are characterized by flow conditions that differ with respect to the threshold of movement of the bed particles, either the ratio τ/τ_{*cr} or the Froude number has to be introduced into the flow resistance law.

For the testing of the relationship between the ratio τ/τ_{*cr} and F, field data gathered from 43 river reaches of Calabria (Colosimo et al. 1988) were also used. The analysis confirmed that τ/τ_{*cr} and F are linearly correlated with a correlation coefficient equal to 0.6.

APPENDIX. REFERENCES

Afzalimehr, H., and Anctil, F. (2000). ''Accelerating shear velocity in gravel-bed channels.'' *J. Hydrol. Sci.*, 45(1), 113–124.

Baiamonte, G., Ferro, V., and Giordano, G. (1995). ''Advances on velocity profile and flow resistance law in gravel bed rivers.'' *Italian contributions to the field of hydraulic engineering*, Vol. 9, 41–89.

Barenblatt, G. I. (1987). *Dimensional analysis*, Gordon & Breach, Science Publishers, Amsterdam, The Netherlands.

Graf, W. H. (1984). *Hydraulics of sediment transport*, Water Resources Publications, Littleton, Colo.

Judd, H. E., and Peterson, D. F. (1969). ''Hydraulics of large bed element channels.'' *Rep. No. PRWG 17-6*, Utah Water Research Lab., Utah State University, Logan, Utah.

Kirinoto, B. A., and Graf, W. H. (1995). ''Turbulence characteristics in rough non-uniform open-channel flow.'' *Proc., Instn. Civ. Engrs.*, Water, Maritime & Energy, 112, 336–348.

Neill, C. R. (1967). ''Mean-velocity criterion for scour of coarse uniform bed material.'' *Proc., XII Int. Assoc. of Hydr. Res.*, Vol. 3, paper C6.

Song, T., and Graf, W. H. (1984). ''Non-uniform open channel flow over a rough bed.'' *J. Hydrosci. Hydr. Engrg.*, 12(1), 1–25.

Thompson, S. M., and Campbell, P. L. (1979). ''Hydraulics of large channel paved with boulders.'' *J. Hydr. Res.*, Delft, The Netherlands, 17(4).

APPLICATION OF 3D MOBILE BED, HYDRODYNAMIC MODEL[a]

Discussion by C. B. Singh[7] and L. K. Ghosh[8]

The recently developed mobile bed version of CH3D, CH3D-SED is well suited for investigation of sedimentation

[a]July 1999, Vol. 125, No. 7, by Daniel Gessler, Brad Hall, Miodrag Spasojevic, Forrest Holly, Hasan Pourtaheri, and Nolan Raphelt (Paper 16668).

[7]Chf. Res. Ofcr., Mathematical Modelling Ctr., Central Water and Power Research Station, Khadakwasla, Pune 411 024 (MS), India. E-mail: wapis@mah.nic.in

[8]Joint Dir., Mathematical Modelling Ctr., Central Water and Power Research Station, Khadakwasla, Pune 411 024 (MS), India. E-mail: wapis@mah.nic.in

in bends, thalweg crossing between bends, and distributaries in sand bed rivers. The model is also capable of simulating freshwater and saltwater interfaces, thermal diffusion, and contaminant transport. The paper describes the validation and application of CH3D-SED for simulating hydrodynamics and sediment transport at several reaches of the Mississippi river.

The governing equations (1)–(4) used in the model are based on a hydrostatic pressure assumption in which a σ stretched approximation is used in the vertical direction. The vertical momentum diffusion coefficient is calculated by

$$A_z = C_v \frac{k^2}{\varepsilon} \tag{36}$$

where a k-ε turbulent eddy viscosity model is represented by (6) and (7). Eqs. (6) and (7), representing the k-ε model, neglect many terms—such as differential derivative terms of x and y in R.H.S. and z in L.H.S.—as compared to the k-ε model used in Huang and Spaulding (1995). Two aspects need to be clarified: (1) whether these approximations are likely to affect the accuracy of simulation of hydrodynamics; and (2) whether the proposed k-ε model takes into account some anisotropic effects appearing in shallow curved channel (i.e., streamline) curvature and the damping effects of free surface and solid walls. The modified k-ε model reported by Ye and McCorquodale (1998) accounts for these effects.

The 10 sigma layers in vertical directions are used. Though the widely used fixed-grid sigma transformation

$$\sigma = \frac{z - \eta}{\eta + h} \tag{37}$$

can address the temporal variation of tidal elevation and irregular bathymetry, it cannot well simulate the sharp fluctuations of concentration profiles near the bed. The fixed σ grids, in which the grid size maintains a constant interval irrespective of water depth, simulate poorly the sharp variation of concentration in deep waters due to large grid size. When large bathymetric irregularities exist, the layer thickness is largest in deep water regions and smallest in shallow water areas. For this reason Huang and Spaulding (1995) employed the γ transformation to get higher resolution for pollutant transport in their 3D surface discharge modeling:

$$z = \left(\gamma - a \frac{D}{D_r} \sin 2\pi\gamma\right) D + \eta \tag{38}$$

where a is constant taken between 0 and 1; η = surface elevation; $D = h + \eta$; h = local water depth; and D_r is a depth scaling parameter and must be larger than $2\pi D_{\max}$, where $D_{\max}$ is the maximum water depth. Though the γ coordinate system kept more grid points on the surface layer, it could not simulate well the sharp concentration profiles at the bottom. Lu (1997) developed a SAG coordinate system in which grids are automatically adjusted according to solution of the local concentration and refined at the region in the high vertical concentration variation to describe net entrainment and net deposition of sediment transport:

$$n_{\text{SAG}} = \frac{z + h + \mu}{\eta + h + m} \tag{39}$$

where η and h = tidal elevation and depth from M.S.L., respectively.

$$\mu = \int_{-h}^{z} \beta |C_{,z}| \, dz \tag{40}$$

$$m = \int_{-h}^{\eta} \beta |C_{,z}| \, dz \tag{41}$$

It is evident that the σ transformation is a special case of above transformation if β = 0. The grid convergence can be adjusted by the attractive (β) in the SAG coordinate system. The larger the attractive coefficient β, the more the grid points will be allocated where higher concentration gradient exists.

The numerical technique used in the external mode of the CH3D-HYD model is based on Leendterse (1967). This model gives an ADI inexactitude as reported by Weare (1979) and Wilders et al. (1988), especially in the case of a dredged channel aligned at 45°. The curvilinear grid lines follow the boundary of the river, whereas the dredged channel is not along the boundary of the river. How is this type of ADI inexatitude avoided in Fig. 6, on page 743? Although in the case of river problem this may not produce much error, this will certainly reduce the limit of the CFL number. Figs. 7–16 (pp. 744–747) represent the hydrodynamic and sediment transport variables that compare the computed results against the observed ones (differences being 10–25%). This difference could be somewhat reduced by using the quasi-hydrostatic 3D model, as reported in Casulli and Stelling (1998). These discrepancies of observed and computed value might be more when it is to be applied to estuarine circulation for predicting an erosion and deposition pattern for long-term simulation.

In view of the ASCE task committee on validation (Wang and Jia 1996), the model is required to be verified analytically and experimentally.

In developing a 3D numerical model of sediment transport processes, a necessary first step is to apply the model to simpler flow situations for which an analytical solution and laboratory measurement exist. For this, four test examples (two analyticals and two experimentals) should be first taken to test the model performance and its accuracy (Lin and Falconer 1996).

1. Hydrodynamic model: analytical and experimental validation. Although a part of analytical validation (case of spherical annular basin and circular island) of CH3D-HY is shown in Sheng (1987), the analytical and experimental validation of vertical behavior of the hydrodynamic model is not found anywhere. The analytical validation can be done in a manner similar to that given in Li and Zhan (1998), whereas experimental validation is given in Huang and Spaulding (1995).
2. Sediment transport model: analytical and experimental validation [refer to Lin and Falconer's (1996) Figs. 2–5].
   a. Analytical test case 1: equilibrium concentration profile (balance between turbulent exchange and settling due to fall velocity):

$$\left(W_s C + \varepsilon_z \frac{\partial C}{\partial z} = 0\right) \tag{42}$$

   b. Analytical test case 2: net entrainment at the bed (balance among horizontal flux, vertical flux, and turbulent exchange in vertical direction):

$$\left[U \frac{\partial C}{\partial x} = \frac{\partial}{\partial z}\left(\varepsilon_z \frac{\partial C}{\partial z}\right)\right] + Ws \frac{\partial C}{\partial z} \tag{43}$$

   The model also needs to be calibrated with laboratory measurements.
   c. Experimental test case 3: net entrainment at the bed
   d. Experimental test case 4: zero entrainment at the bed. For details, Figs. 4 and 5 of Lin and Falconer (1996) may be referred to.

The sediment transport model, which is a combination of the two-dimensional Exner equation [(16)], the advection dis-

persion equation of suspended sediment [(17)], and the bed load model developed by Van Rijn [(21)], is a very good representation of the Mississippi river, but it requires a modeling effort when it is applied to a coastal area that is highly nonlinear and unsteady with respect to tidal hydrodynamics and sediment transport.

While applying CH3D-SED to the Mississippi river, the stability of the model, such as the Courant number for the hydrodynamic part, is not discussed. Similarly, the Peclet number, which is a criteria of stability for modeling advection and dispersion equation, is not at all discussed. The future scope of the model lies in the application of the full 3D model for hydrodynamics and transport in the case of the Mississippi river.

APPENDIX. REFERENCES

Casulli, V., and Stelling, G. S. (1998). ''Simulation of curved open channel flow by three dimensional Quasi-hydrostatic, free surface flow.'' *J. Hydr. Engrg.*, ASCE, 124(7), 687–698.

Huang, W., and Sapulding, M. (1995). ''3D model of estuarine circulation and water quality induced by surface discharges.'' *J. Hydr. Engrg.*, ASCE, 121(4), 300–311.

Leendertse, J. J. (1967). ''Aspects of a computational model for long period water wave propagation.'' *RM-5294-PR*, The Rand Corporation.

Li, Y. S., and Zhan, J. M. (1998). ''Three-dimensional finite element model for stratified coastal seas.'' *J. Hydr. Engrg.*, ASCE, 124(7), 699–703.

Lin, B., and Falconer, R. A. (1996). ''Numerical modelling of three-dimensional suspended sediment for estuarine and coastal waters.'' *J. Hydr. Res.*, Delft, The Netherlands, 34(4), 435–456.

Lu, Q. (1997). ''3D numerical modelling of sediment transport with a new solution adaptive grid technique.'' *Proc., 27th Congr. of IAHR*, ASCE, New York, 25–31.

Sheng, P. (1987). ''On modelling three-dimensional estuarine and marine hydrodynamics.'' *Three-dimensional model of marine and estuarine dynamics*, J. C. J. Nihoul and B. M. Jamart, eds., Elsevier, Amsterdam, 35–53.

Wang, S. Y., and Yafer, J. (1996). ''Verification and refinement of free surface flow model.'' *Environmental and coastal hydraulics*, ASCE, New York, 853–869.

Weare, T. J. (1979). ''Errors arising from irregular boundaries in ADI solutions of the shallow-water equations.'' *Int. J. Numer. Methods in Engrg.*, 14, 921–931.

Wilders, P., Van Stijn, G. S., Stelling, G. A., and Fokkema. (1988). ''A fully implicit splitting method for accurate tidal computations.'' *Int. J. Numer. Methods in Engrg.*, 26, 2707–2721.

Ye, J., and McCorquodale, J. A. (1998). ''Simulation of curved open channel flow by three-dimensional hydrodynamic model.'' *J. Hydr. Engrg.*, ASCE, 124(7).

CHARACTERISTICS OF SKIMMING FLOW OVER STEPPED SPILLWAYS[a]

Discussion by Robert M. Boes[3]

INTRODUCTION

The authors are to be congratulated for their comprehensive model study on two-phase cascade flow using different slopes and step heights in a large model flume. In contrast to most previous model studies, their large model size allows to minimize scale effects. A true similarity cannot be achieved for two-phase flow, however, because the Froude, Reynolds, and Weber-similarity laws would have to be satisfied simultaneously. Air bubbles are proportionally too large, resulting in a lower transport capacity and a higher detrainment rate as compared with the prototype (Kobus 1984). As scale effects can be estimated by using model families, the discusser would like to know if the results for different model steps on air concentrations and flow velocities of the air-water mixture have been compared, and if scale effects were detected.

The discusser conducted model tests on skimming flow in a large model of a stepped spillway for two slopes, 1.73:1 (30°) and 0.84:1 (50°), with y_c/h in the range of 0.8 to 10.5. Steps of height h = 92.4, 46.2, and 23.1 mm were used for the flatter slope, and of h = 93.3 and 31.1 mm for the steeper model. For a minimum approach flow depth y_o = 24 mm, no major discrepancies between different model scales were found. For large Reynolds and Weber numbers, the two-phase flow can thus be adequately modeled according to the Froude similarity law. The following remarks and questions are further raised.

VELOCITY DISTRIBUTION

When comparing the authors' typical velocity profile, Fig. 3(b), with the discusser's data, a significant deviation is observed for distances $y > y_{um}$ normal to the virtual bed. A typical velocity profile as measured by the discusser is shown in Fig. 11. A novel fiber-optical instrumentation was used to simultaneously measure both local air concentrations and flow velocities. Boes and Hager (1998) give a detailed description of this measurement technique. Whereas the discusser's velocity profiles increase continuously up to some distance normal to the virtual bed and remain quasi-constant as y increases further, similar to Tozzi (1994), there is a sharp reduction of flow velocities for distances larger than y_{um} for the authors' data. This decrease in u_m for $y > y_{um}$ presumably occurs because of an inaccurate velocity measuring method, because the use of a Prandtl tube is questionable for highly aerated flows. The authors state that there was agreement between velocity measurements by means of high-speed photography and the Prandtl tube *in the lower region*. As the boundary between the lower and upper region is defined by the transition depth y_T, which is always equal to or smaller than y_{um}, the deviation from the discusser's data clearly occurs in the *upper* region. Although $y_{0.9}$ is the accepted characteristic mixture flow depth for two-phase flow down spillways, the discusser performed measurements to an upper limit $y_{ul} = y_{0.99} = y(C = 0.99)$. A

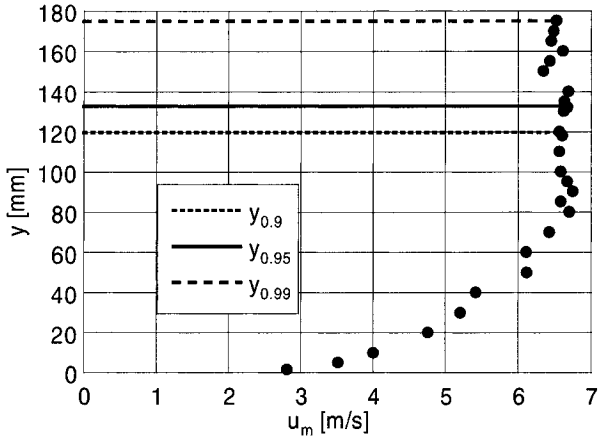

FIG. 11. Typical Velocity Profile in Fully Developed Skimming Flow (l/h = 0.84, h = 93.3 mm, and y_c/h = 2.4)

[a]April 1999, Vol. 125, No. 4, by M. R. Chamani and N. Rajaratnam (Paper 17002).

[3]PhD Student, Lab. of Hydraulics, Hydrol. and Glaciology (VAW), Fed. Inst. of Technol. (ETH), CH-8092 Zurich, Switzerland.

slight decrease in local velocity values may be observed only in the highly aerated flow region with $y > y_{0.95}$ (Fig. 11).

The discusser's u_m-data follow a power law, in close agreement with smooth chute flows (Cain 1978; Wood 1985), i.e., $U_{0.9} = Y_{0.9}^{1/6.3}$, with $U_{90} = u_m/u_{0.9}$ and $Y_{0.9} = y/y_{0.9}$. The accuracy of the concentration and velocity data was checked with the clear water discharge q as

$$q = \int_0^{y_{ul}} (1 - C)u_m \, dy \tag{22}$$

to only up to 6% deviation. The error decreased when y_{ul} was increased to $y_{ul} = y_{0.99}$, because practically the whole water discharge was detected. Did the authors perform similar checks?

Further questions on the velocity distribution are, How did the authors determine the *local* and the *average* densities ρ_m and $\bar{\rho}_m$, respectively, of the air-water mixture? The discusser proposes to compute $\rho_m = \rho_w(1 - C)$ and $\bar{\rho}_m = \rho_w(1 - \bar{C})$ with C as local air concentration and $\bar{C}$ as depth-averaged concentration according to (7). In this case, the shear velocity u_* between the main flow and the recirculating vortices in the step cavities would be $u_* = \sqrt{g \sin \theta y_{0.9}(1 - \bar{C})/(1 - C_b)}$, where C_b is the close-to-bottom air concentration. To obtain agreement between u_* as given by the authors and calculated from the previous equation would require C_b-values much in excess of those observed. How was the equivalent roughness k_s determined? Was it found by fitting u_m/u_* versus y_ε/k_s to (13)?

DEPTH-AVERAGED AIR CONCENTRATION

In Fig. 12, the authors' data on the mean air concentration $\bar{C}$ are compared with those of the discusser for a similar slope of 0.84, computed on the basis of (7). Agreement results only for the smallest discharges tested, whereas the discusser's data suggest significantly more air content than proposed by the authors for larger dischargers. The reason for this discrepancy can be twofold: different measuring devices, or the flow in the authors' experiments was not fully developed. Even in the discusser's model study with a vertical model height of 4.2 m, the flow was not fully developed for the highest discharges and large steps. However, essentially equal air concentration and velocity profiles occurred at the end of the authors' flume. The discusser assumes that the authors' electrical concentration probe was less suitable for highly aerated, high-speed two-phase flow than the fiber-optical instrumentation, because of (1) the large size of the sample volume compared to a probe tip diameter of approximately 100 μm, and (2) a significantly lower scan rate. Both arguments suggest an underestimation of air concentration, because air bubbles are either deviated by the probe tip or remain undetected due to the limited electronic sampler frequency.

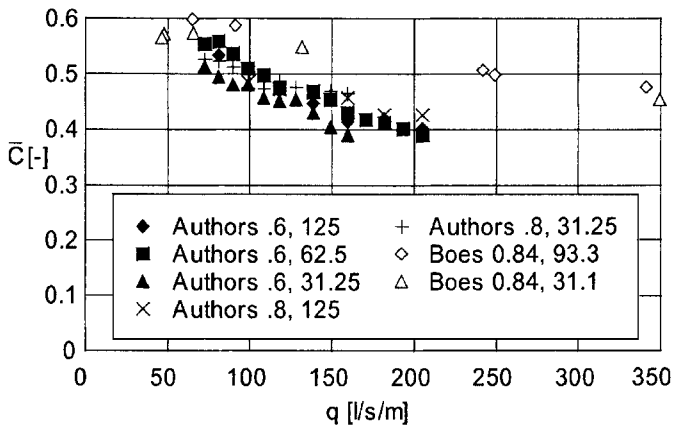

FIG. 12. Variation of $\bar{C}$ with q

SKIN FRICTION COEFFICIENT

Fig. 13 compares the authors' data from Fig. 8(b) with those of the discusser, where $Y = y_{0.9}$. The friction coefficient was calculated in two ways: first, from (15), second, from (15) with the clear water depth $y_w = (1 - \bar{C})y_{0.9}$, instead of $y_{0.9}$. The agreement of the data computed from (15) with the authors' data is quite good, but the general trend of (2) and (16) is questionable, because the discussers' results seem to suggest, rather, a decrease of the friction coefficient with increasing relative roughness k/Y. This behavior is also observed for the authors' data and those of Bayat (1991) in Fig. 8(a), with approximately parallel lines for different step heights. Whereas for chute inclination angles $\theta \leq 45°$ the friction coefficient increases with increasing k/Y, in analogy to the classical data of Nikuradse, the converse occurs for $\theta > 45°$. A similar resistance phenomenon on stepped spillways was also described by Yildiz and Kas (1998) for inclination angles $\theta = 30°$ and 51.3°. If the clear water depth y_w is considered, the friction coefficients are significantly smaller than calculated from (15), as can be seen in Fig. 13. In the discusser's opinion, friction coefficients should be computed based on clear water depths to avoid overestimation of head losses taking place on cascades. Given the low density of the gas phase of about 1/800 of pure water, aeration can be neglected in the calculation of Reynolds shear stress, (10), and only the clear water portion of the two-phase flow is accounted for. If y_w instead of $y_{0.9}$ were also considered for the relative roughness, the solid data points in Fig. 13 would be shifted to the right, i.e., toward larger k/Y-values.

ENERGY DISSIPATION

In the authors' equations (18) and (19), the Coriolis coefficient α was used in combination with mean velocity of the air-water mixture V_m. This suggests that $V_m = q/y_{0.9}$, i.e., V_m is calculated from continuity rather than by integrating the measured velocity profiles, because α already accounts for the velocity distribution. If velocities are computed from continuity, then y_w instead of $y_{0.9}$ should be taken as the reference flow depth, analogous to friction coefficient calculations. What α-values did the authors obtain from their u_m-profiles? Was V_m in (15) also determined from continuity? In this case (15) would become $c_f = 2gy_{0.9}^3 \sin \theta/q^2$. For the discusser's data in Fig. 14,

$$V_m = \frac{1}{y_{0.9}} \int_0^{y_{0.9}} u_m \, dy \tag{23}$$

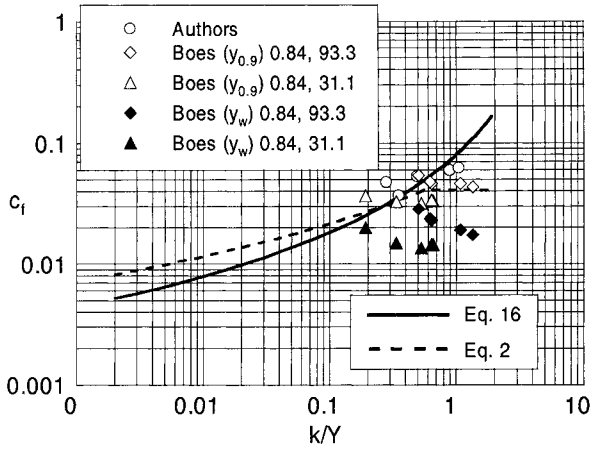

FIG. 13. Variation of Average Skin Friction Coefficient with k/Y

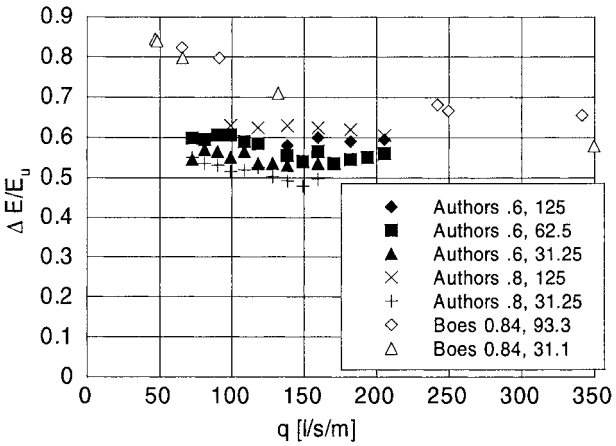

FIG. 14. Relative Energy Dissipation for Skimming Flow for Stepped Spillway Models

For the purpose of comparison, the discusser's data for head losses $\Delta E/E_u$ were added to the authors' Fig. 9, with V_m from (23) and the piezometric head $y_w \cos \theta$. Surprisingly, the authors' results suggest energy losses that are significantly smaller than the discusser's for a given discharge (Fig. 14). The opposite would have been expected for $V_m = q/y_{0.9}$ in (19). This further raises the question on how V_m was determined, and on the reliability of the u_m-measurements. It would be interesting to compare the authors' V_m-values as a function of step height, slope, and discharge with the data of the discusser. It can also be noted that the authors' data, especially for h/l = 0.8, depend more on the step height than those of the discusser.

APPENDIX. REFERENCES

Bayat, H. O. (1991). "Stepped spillway feasibility investigation." *Proc., 17th ICOLD Congr.*, Vienna, Austria, Q.66(R.98), 1803–1817.

Boes, R. M., and Hager, W. H. (1998). "Fiber-optical experimentation in two-phase cascade flow." *Proc., Int. RCC Dams Seminar*, K. Hansen, ed., Denver, Colo.

Cain, P. (1978). "Measurements within self-aerated flow on a large spillway." PhD thesis, Ref. 78-18. University of Canterbury, Christchurch, New Zealand.

Kobus, H. (1984). "Local air entrainment and detrainment." *Proc., Symp. on Scale Effects in Modelling Hydraulic Structures*, H. Kobus, ed., Esslingen, Germany, 4.10, 1–10.

Tozzi, M. J. (1994). "Residual energy in stepped spillways." *Int. Water Power & Dam Constr.*, 46(5), 32–34.

Wood, I. R. (1985). "Air water flows." *Proc., 21st IAHR Congr.*, International Association of Hydraulic Research, Delft, The Netherlands, 6, 18–29.

Yildiz, D., and Kas, I. (1998). "Hydraulic performance of stepped chute spillways." *Hydropower & Dams*, 5(4), 64–70.

Discussion by Hubert Chanson[4]

The discusser wishes to congratulate the authors for their authoritative paper. He believes that the work is a necessary addition to the topic of stepped spillway flow.

The paper presents a true systematic study of skimming flow. Important outcomes include a characterization of free-surface aeration and flow measurements in a large-size facility. Up to now, too little attention has been paid to the scale effects in stepped spillway studies. Although open channel flows are commonly modeled with a Froude similitude, similarity of stepped channel flows is more complex because of the various flow regimes (nappe and skimming flow regime), the role of the steps in enhancing turbulent dissipation, and the substantial amount of free-surface aeration (Chanson 1997b). The contradicting results obtained by various stepped model studies, all supposed to be in Froude similitude, reflect the complexity of stepped spillway flows and the limitations of the Froude similitude. Indeed BaCaRa (1991, 1997) described a systematic laboratory investigation of the M'Bali dam spillway. Several identical models were built with the geometric scales of 1/10, 1/21.3, 1/25, and 1/42.7 and all in Froude similitude. For the scales 1/25 and 1/42.7, the experimental results showed that the developing flow properties and the flow resistance were not correctly reproduced. The authors' results are less subject to scale effects than most because they were performed with a large-size model.

The authors' results highlight the significant air entrainment taking place above stepped spillway. Practically professional engineers must take into account free-surface aeration in their design. The discusser (Chanson 1993, 1994) argued that free-surface aeration affects the design because of flow bulking and drag reduction. The characteristic depth $y_{0.9}$ (where $C = 0.90$) accounts the flow bulking caused by the air entrainment and it must be used as a design parameter for the height of the chute sidewalls. Drag reduction, induced by free-surface aeration, results from the interactions between the entrained air bubbles and the turbulence next to the invert. For smooth spillway chutes, it may be estimated as

$$\frac{(C_f)_e}{C_f} = 0.5 \cdot \left(1 + \tanh\left(0.628 \cdot \frac{0.514 - \bar{C}}{\bar{C} \cdot (1 - \bar{C})}\right)\right) \qquad (24)$$

where C_f = clear-water friction coefficient; $(C_f)_e$ = air-water flow friction coefficient; and $\bar{C}$ = mean air concentration (e.g., Chanson 1997a). Although there is little information on the validity of (24) to stepped chutes, its use for stepped spillway design is conservative and increases the safety of the structure.

Despite the outstanding insights of the study, the discusser wishes to point two weaknesses: an inadequate analysis of the air entrainment process and some limitations of the velocity probe measurements.

FREE-SURFACE AERATION PROCESS

Although the authors presented important results describing the free-surface aeration, their analysis [(4)–(8)] is inadequate and disappointing. It is based on ancient references that derived from the work of the late Professor Lorenz Straub and his coworkers. The development assumes an air-water flow structure with a lower region consisting of air bubbles distributed through a water flow and an upper flow region with a heterogeneous mixture of water droplets and globules ejected from the stream (Straub and Anderson 1958). In the discusser's opinion, this model does not reflect the physical nature of the air-water flow. Measured air concentration and velocity distributions in open channel flows exhibit smooth continuous functions without marked discontinuity between inner and outer flow regions. The air-water flow behaves as a homogeneous mixture between 0 and $y_{0.9}$ (e.g., Wood 1991; Chanson 1997a). A more physical model was proposed by Wood (1984) based upon the conservation equation for the mixture density in the equilibrium region. Wood's model fits well with experimental data for mean air contents between 100% and 75% (Wood 1984, 1985, 1991), although it includes empirical constants without physical meaning (denoted G′ and B′ in the original paper). Recently, the discusser proposed a new air bubble diffusion model based upon theoretical development that is a good agreement with model and prototype data (Chanson 1995, 1997a).

In uniform equilibrium flows, the continuity equation for air in the air-water flow yields

[4]Sr. Lect. in Fluid Mech., River and Coast. Hydr. and Envir. Engrg., Dept. of Civ. Engrg., Univ. of Queensland, Brisbane QLD 4072, Australia.

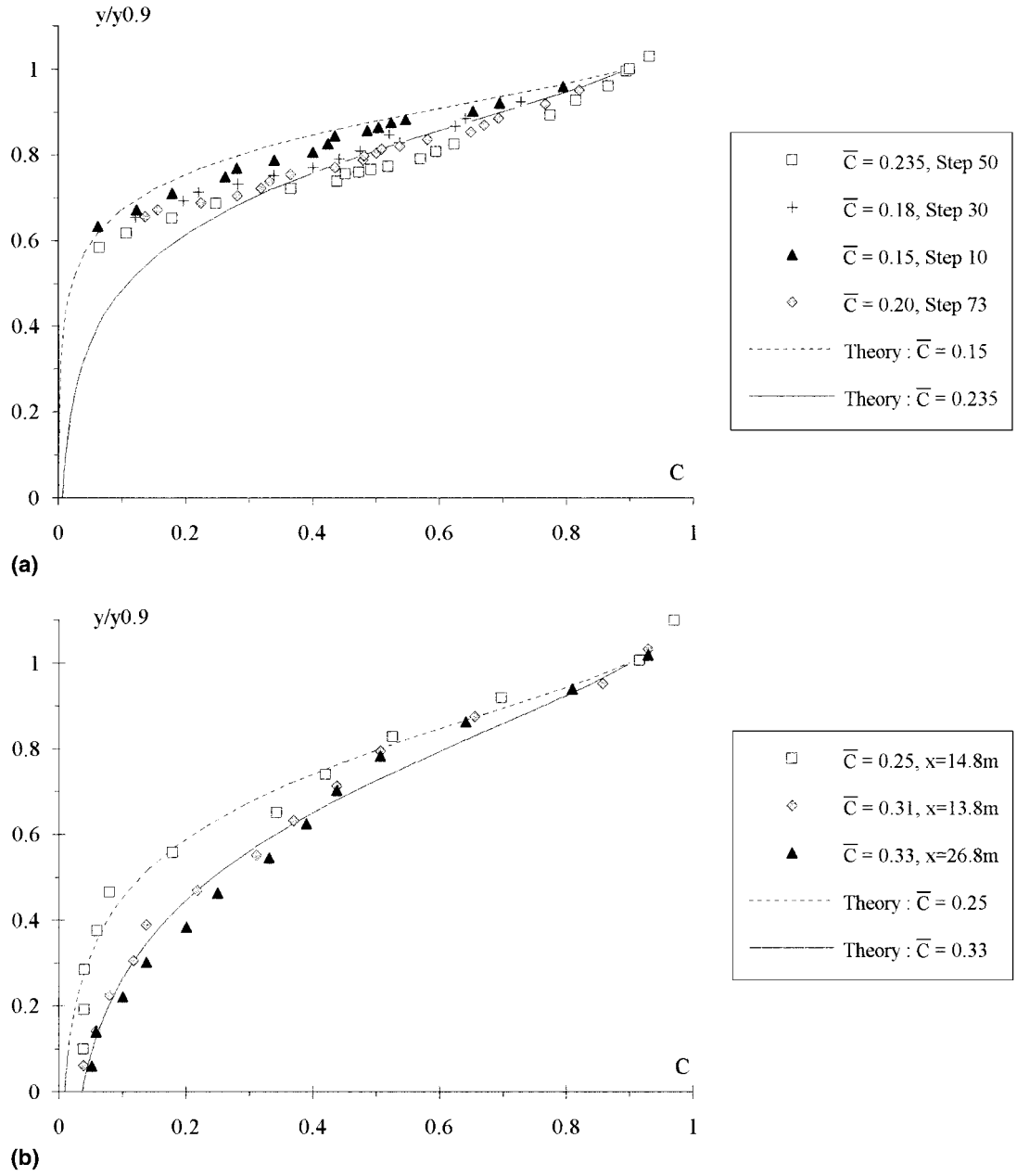

FIG. 15. Air Concentration Distributions in Stepped Chutes with Skimming Flow: (a) Measurements at Brushes Clough Dam Spillway (Baker 1994)—Inclined Downward Steps (h = 0.19 m, $\delta = -5.6°$), θ = 18.4°; (b) Ruff and Frizell (1994): q = 2.6 m²/s, θ = 26.6°, Inclined Downward Steps (h = 0.154 m)

$$\frac{\partial}{\partial y}\left(D_t \cdot \frac{\partial C}{\partial y}\right) = (u_r)_{\text{Hyd}} \cdot \cos\theta \cdot \frac{\partial}{\partial y}\left(C \cdot \sqrt{1 - C}\right) \qquad (25)$$

where D_t = turbulent diffusivity in the direction normal to the flow direction, and where $(u_r)_{\text{Hyd}}$ is the rise velocity in hydrostatic pressure gradient [Eq. (25) implies that the bubble rise velocity in a two-phase flow mixture is a function of the void fraction C and rise velocity in hydrostatic pressure gradient.] The integration of (24) gives

$$C = 1 - \tanh^2\left(K' - \frac{y}{2 \cdot D' \cdot y_{0.9}}\right) \qquad (26)$$

where K' is an integration constant; $D' = [D_t/(u_r)_{\text{Hyd}} \cdot \cos\theta \cdot y_{0.9})$; and $\tanh(x) = (\exp(+x) - \exp(-x))/[\exp(+x) + \exp(-x)]$ (Chanson 1995, 1997a). K' is an integration constant that is deduced from the boundary condition C = 0.9 for $y = y_{0.9}$:

$$K' = \text{than}^{-1}(\sqrt{0.1}) + \frac{1}{2 \cdot D'} \qquad (27)$$

If the diffusivity is unknown, it can deduce from the mean air content:

$$\bar{C} = 2 \cdot D' \cdot \left(\tanh\left(\tanh^{-1}(\sqrt{0.1}) + \frac{1}{2 \cdot D'}\right) - \sqrt{0.1}\right) \qquad (28)$$

Eq. (28) was validated with smooth-invert open channel flows. It is also in good agreement with stepped spillway flows, including the authors' work (Fig. 15). In Fig. 15, the analytical solution [(26)] is compared with data obtained on large models (Ruff and Frizell 1994; Chamani and Rajaratnam) and prototype (Baker 1994). (For completeness: the caption of the authors' Fig. 3(a) is incorrect. It should be l/h = 0.6, y_c/h = 1.3 to give $y_{0.9}$ = 99 mm.)

Note that (26) describes physically the air concentration distribution as a function of two parameters only, namely, $y_{0.9}$ and

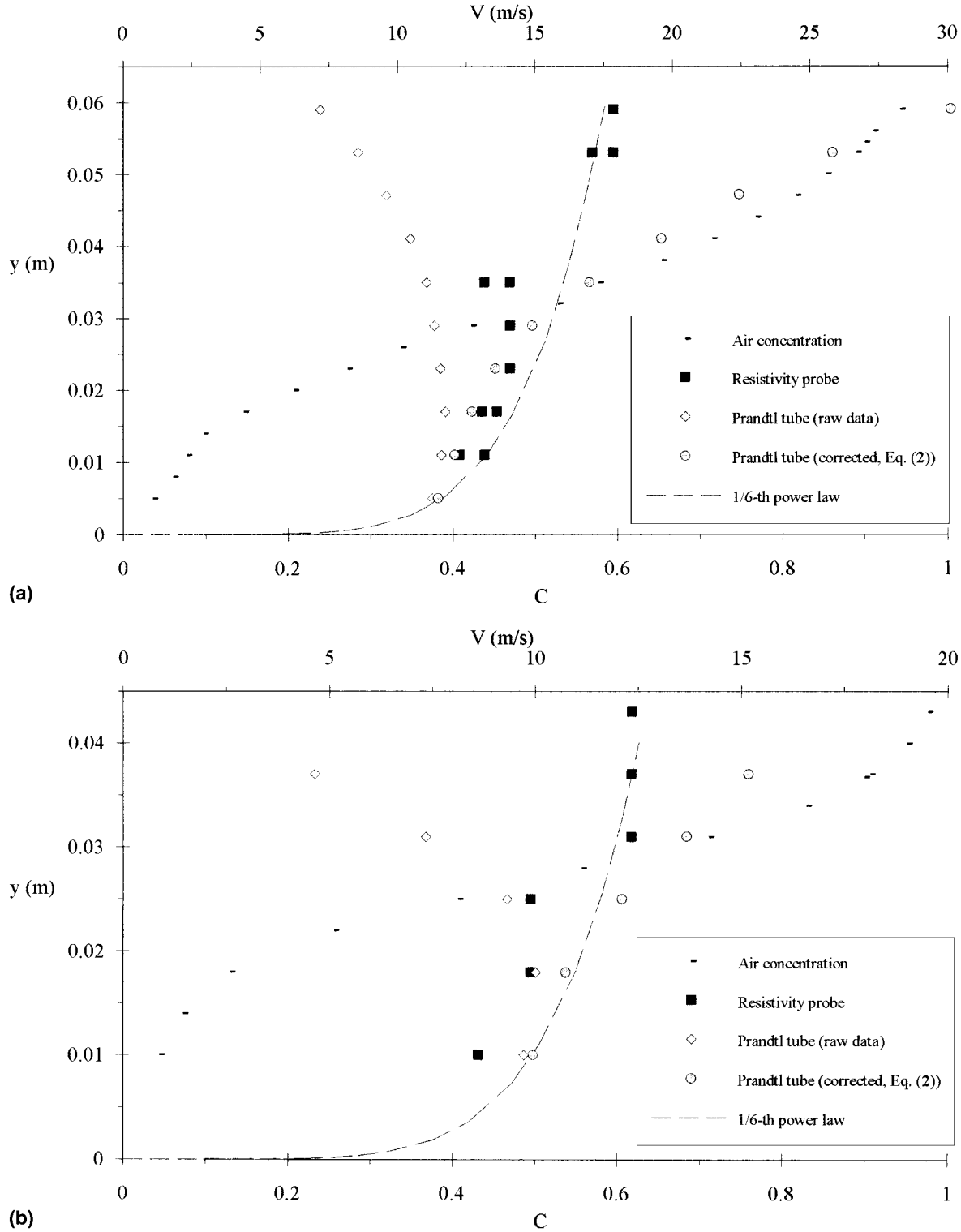

FIG. 16. Velocity Distribution Data Measured with Prandlt Tube and Dual-Tip Resistivity Data: (a) $q = 0.40$ m²/s, $\bar{C} = 0.41$, $\theta = 52.3°$; (b) $q = 0.27$ m²/s, $\bar{C} = 0.30$, $\theta = 5.23°$; (c) Chamani and Rajaratnam: $q = 0.205$ m²/s, $\theta = 59°$, $h = 0.125$ m

$\bar{C}$ (or $y_{o.0}$ and D'). It is a simplification compared to earlier models—e.g., at least six parameters are required to describe the void fraction distribution in Straub and Anderson's model.

VELOCITY MEASUREMENT IN AIR-WATER FLOWS

Velocity measurements in air-water flows is difficult, and the discusser's experience (e.g., Chanson 1997a) suggests that the authors' (3) cannot estimate accurately the time-averaged velocity in the upper flow region. Indeed, classical measurement devices (e.g., pointer gauge, Prandtl-Pitot tube) give inaccurate readings in bubbly flows because the air bubbles and bubble interfaces interfere with the probe. The discusser conducted a series of comparative tests in self-aerated flows (smooth invert) using a Prandtl tube (Ø = 3.3 mm, 1 mm stagnation hole Ø) and some dual-tip resistivity probes (Ø = 200-μm and 25 mm inner electrode) mounted side by side. (Note that the resistivity probe sensors were 50 and 400 times smaller than the air concentration probe sampling volume used by the authors.) The Prandtl tube data included the velocity and the standard deviation of the velocity fluctuations. The outputs of the dual-tip resistivity probes comprised the air con-

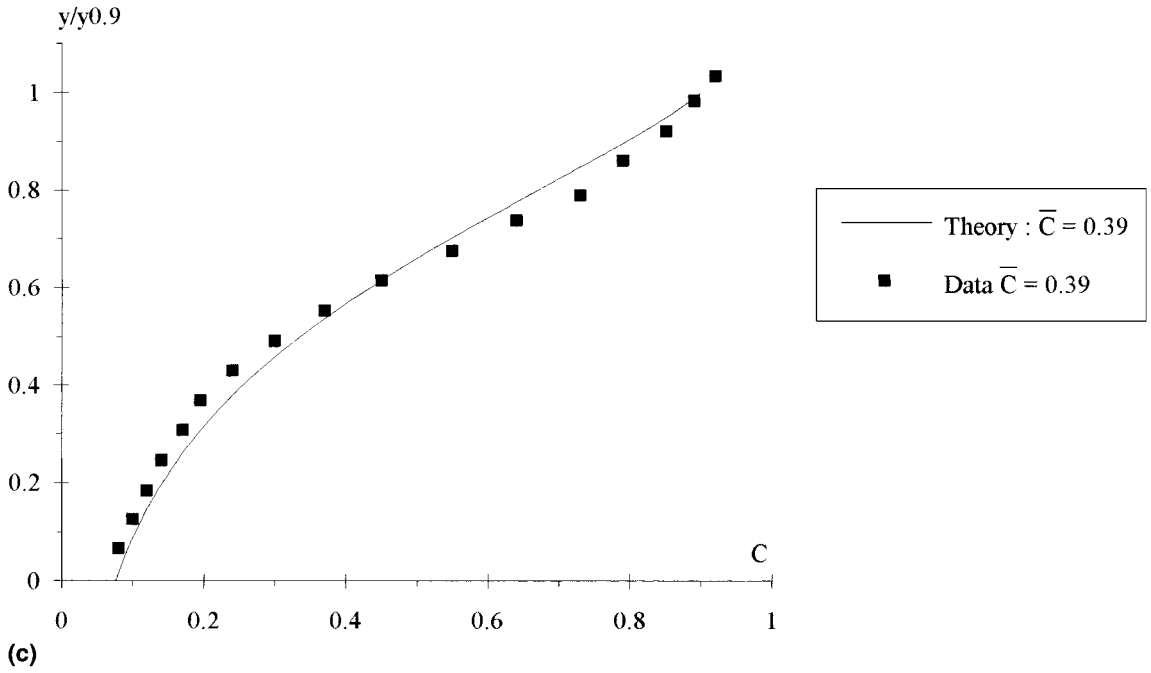

FIG. 16. (*Continued*)

centration, air-water velocity, bubble count rate, bubble size distributions, and air-water interfacial area. A comparative analysis of the velocity distribution data shows that the Prandtl tube data (raw data) underestimate the air-water velocity for void fraction larger than 0.10 to 0.20, while corrected data [authors' (3)] gives nonmeaningful results in the upper region ($C > 0.5$ to 0.6) (Fig. 16). A typical example is presented in Fig. 16, showing resistivity probe data (black square), raw Prandtl tube data (white diamond), and Prandtl tube data corrected by the authors' (3) (grey circle) and a 1/6th power law distribution satisfying the continuity for water.

Air-water flow properties must be recorded by more sophisticated means than a Prandtl-Pitot tube. Earlier investigations used photographic techniques, gamma-ray absorption probes, and light-scattering systems, for example. Newer measurement systems were developed successfully, including small resistivity probes, conical hot-film probes, optical probes, and Fiber Phase Doppler Anemometer (FPDA). A combination of two (or more) techniques can be combined also. Authoritative reviews on two-phase flow measurement systems include Cartellier and Achard (1991), Bachalo (1994), and Chanson (1997a).

ACKNOWLEDGMENTS

The discusser thanks R. Baker and P. Royet for providing him with their experimental data.

APPENDIX I. REFERENCES

BaCaRa. (1991). "Etude de la dissipation d'energie sur les evacuateurs à marches." ('Study of the energy dissipation on stepped spillways.') *Rapport d'Essais*, Projet National BaCaRa, CEMAGREF-SCP, Aix-en-Provence, France (in French).

BaCaRa. (1997). "Roller compacted concrete: RCC for dams." *Presses de l'Ecole Nationale des Ponts et Chaussées*, Paris.

Bachalo, W. D. (1994). "Experimental methods in multiphase flows." *Int. J. Multiphase Flow*, Vol. 20, Suppl., 261–295.

Baker, R. (1994). "Brushes clough wedge block spillway—progress report no. 3." *SCEL Proj. Rep. No. SJ542-4*, University of Salford, U.K.

Cartellier, A., and Achard, J. L. (1991). "Local phase detection probes in fluid/fluid two-phase flows." *Rev. Sci. Instrum.*, 62(2), 279–303.

Chanson, H. (1993). "Stepped spillway flows and air entrainment." *Can. J. Civ. Engrg.*, Ottawa, 20(3), 422–435.

Chanson, H. (1995). "Air bubble diffusion in supercritical open channel flow." *Proc., 12th Australasian Fluid Mechanics Conference*, R. W. Bilger, ed., AFMC, Sydney, Australia, Vol. 2, 707–710.

Chanson, H. (1997a). *Air bubble entrainment in free-surface turbulent shear flows*, Academic, London.

Chanson, H. (1997b). "Discussion of 'model study of a roller compacted concrete stepped spillway.'" *J. Hydr. Engrg.*, ASCE, 123(10), 931–933.

Ruff, J. F., and Frizell, K. H. (1994). "Air concentration measurements in highly-turbulent flow on a steeply-sloping chute." *Proc., Hydr. Engrg. Conf.*, ASCE, New York, Vol. 2, 999–1003.

Wood, I. R. (1984). "Air entrainment in high speed flows." *Proc., Int. Symp. on Scale Effects in Modelling Hydr. Struct.*, H. Kobus, ed., IAHR, Delft, The Netherlands, paper 4.1.

Wood, I. R. (1985). "Air water flows." *Proc., 21st IAHR Congr.*, International Association of Hydraulic Research, Delft, The Netherlands, Keynote address, 18–29.

Wood, I. R. (1991). "Air entrainment in free-surface flows." *IAHR Hydraulic Structures Design Manual No. 4*, Hydraulic Design Considerations, Balkema, Rotterdam, The Netherlands.

APPENDIX II. NOTATION

The following symbols are used in this paper:

B = integration constant (defined by Wood 1984);
C = local void fraction;
D_t = turbulent diffusivity (m^2/s) of air bubbles in air-water flow;
D' = dimensionless turbulent diffusivity: $D' = D_t/[(u_r)_{Hyd} \cdot \cos\theta \cdot y_{0.9}]$ (after Chanson 1995);
G' = integration constant (defined by Wood 1984);
K' = dimensionless integration constant (after Chanson 1995); and
$(u_r)_{Hyd}$ = bubble rise velocity (m/s) in hydrostatic pressure gradient.

Discussion by Jorge Matos[5]

INTRODUCTION

The authors have presented a new and important contribution to the hydraulics of skimming flow over stepped spill-

[5]Lect., Technical Univ. of Lisbon, IST, Dept. of Civ. Engrg., Lisbon 1096, Portugal.

ways. Based on the results of their laboratory study, topics of relevance such as air entrainment, flow resistance, and energy loss have been addressed.

In this discussion, some of the authors' relevant results and observations are analyzed in light of other data available in the literature, namely on air entrainment (e.g., Lejeune et al. 1995; Matos and Frizell 1997), velocity distribution in highly-aerated flow (Lai 1971; Tozzi 1992; Frizell et al. 1994; Boes and Hager 1998), and flow resistance (Matos and Quintela 1995a).

Because of its relevance for the interpretation of the authors' experimental data, the discussion includes a brief review of previous work dealing with the equilibrium mean air concentration in self-aerated flow on conventional (unstepped) chutes as well as in skimming flow over stepped spillways.

AIR CONCENTRATION DISTRIBUTION AND MEAN AIR CONCENTRATION

In Fig. 3(a), the authors show that the model developed by Straub and Anderson (1958) for the air concentration distribution in self-aerated flow provides by a good agreement with the experimental data gathered in the skimming flow, in particular for $y < y_{0.9}$. This conclusion is in accordance with Matos and Frizell (1997), where it was found that the air concentration distribution in self-aerated flow on conventional chutes is similar to that observed in skimming flow over stepped spillways. In the latter study, the air concentration distribution model of Wood (1984, 1991) has been compared with the experimental data, as illustrated in Fig. 17. From Fig. 17 it can also be observed that (after Matos and Frizell, 1997) (1) the air concentration profiles—in particular, those located near the spillway toe—seem to indicate the presence of an air concentration boundary layer of about 1.5 cm, in conformity with the findings of Chanson (1989) for self-aerated flow on conventional chutes. In this layer, the above mentioned models of Straub and Anderson (1958) and Wood (1984) might not have been able to provide very precise estimates of the local air concentration, namely in the quasi-uniform flow region. And (2) the uniform flow has not been reached in the stepped chute.

The conclusion drawn in the second observation was based upon Wood's (1983) reinterpretation of the experimental data of Straub and Anderson (1958). According to Wood (1983), not all of Straub and Anderson's results were in the equilibrium flow region, which would compromise the validity of the ASCE curve [(20]. Wood (1983) stated also that the gradually varied flow region is one of very slow growth, and therefore it was not surprising that the original measurements of Straub and Anderson were interpreted as being in a region of equilibrium air concentration. Finally, Wood (1983) proposed that the uniform mean air concentration would be a function of the slope only. Even though that proposal might not have been fully consensual (see, e.g., Ahshar et al. 1994), Wood's (1995) discussion has greatly contributed to a better understanding of his view. Therein it was shown that the properties of the point of inception should be largely independent of the Reynolds number and relative roughness, so that the inception Froude number could be replaced by the spillway slope. In Matos (1995), it was also concluded that in uniform self-aerated flow on conventional spillway chutes, the influence of the water discharge and roughness on the Froude number is not expected to be significant when compared with that of the spillway slope.

If one accepts that the roughness of the spillway is not a relevant parameter (even for very high values of k), then the equilibrium mean air concentration in skimming flow would likely be similar to that obtained in self-aerated flow on a conventional chute of equal slope. The analysis of Chanson (1994, pp. 81–84), Ruff and Frizell (1994), Matos and Quintela (1995a), and Matos and Frizell (1997) seem to support the above reasoning. Using the formula proposed by Hager (1991) for the uniform mean air concentration ($\bar{C} = 0.76 \sin \theta^{0.76}$), it yields $\bar{C} = 67\%$ ($l/h = 0.6$) and $\bar{C} = 63\%$ ($l/h = 0.8$).

It appears, therefore, reasonable to judge that the uniform fully aerated flow has not been attained in most of the authors' experimental tests [Fig. 4(a) or Fig. 10(b)]. This conjecture seems to be further supported by the analysis of Fig. 18, in which the experimental data obtained by the authors in the 51.3° sloping chute ($l/h = 0.8$) has also been plotted. Once the dam crest height above the spillway toe (H_d) could not be assessed from the authors' data, this parameter has been assumed equal to the height of the upstream channel bed above the toe (Z_0). Although H_d is obviously slightly greater than Z_0, the general conclusions are expected to remain valid.

From Fig. 18 it might be concluded that (after Matos and Quintela 1995a) (1) for similar values of H_d/y_c and k/D_h [k is the roughness height and $D_h = 4\,d$, where d is the equivalent clear water depth, $d = y_{0.9}(1 - \bar{C})$], the $\bar{C}$ values obtained from the authors' data are of the same order of magnitude of those estimated directly from the data of Lejeune et al. (1995) or indirectly (nonintrusive approach), from Tozzi (1992); (2) a tendency of increase of $\bar{C}$ with H_d/y_c is observed, and for constant H_d/y_c, $\bar{C}$ seem to increase with k/D_h for low values of k/D_h; (3) uniform fully aerated flow conditions might not have

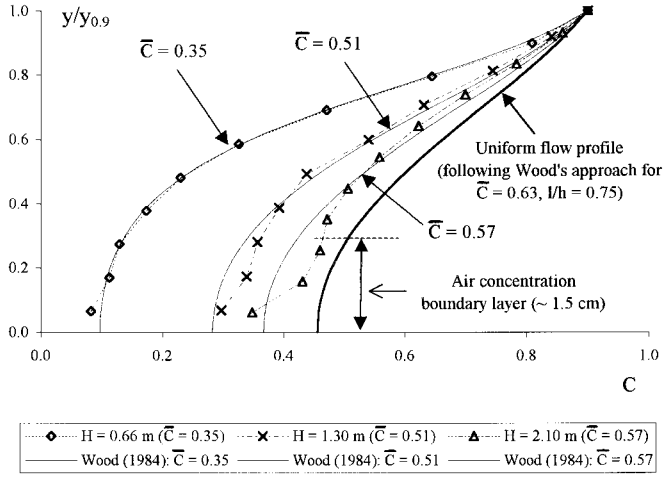

FIG. 17. Air Concentration Distribution in Skimming Flow on Steep Stepped Chute: $\theta = 51.3°$ ($l/h = 0.75$), $h = 8.0$ cm, $q_w = 0.1$ m²/s (after Matos and Frizell 1997)

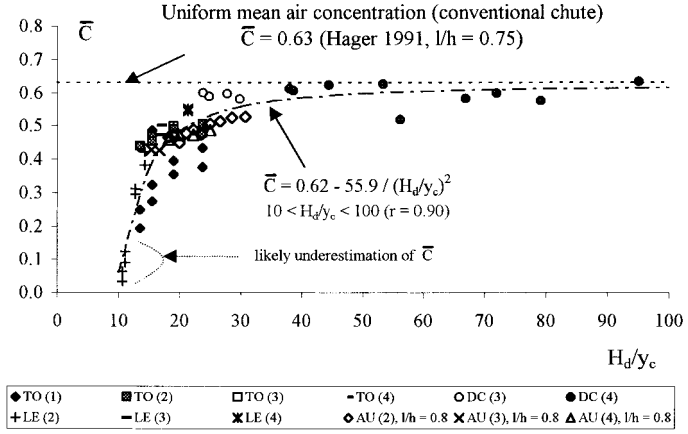

Notes:
TO - Tozzi (1992); DC - Diez-Cascon et al. (1991); Lejeune, Lejeune and Lacroix (1994); AU - Authors
(1) $k/D_h \leq 0.1$; (2) $0.1 < k/D_h < 0.2$; (3) $0.2 < k/D_h \leq 0.3$; (4) $k/D_h > 0.3$.

FIG. 18. Mean Air Concentration in Skimming Flow over Steep Stepped Chutes (after Matos and Quintela 1995a)

been attained for most of the experiments of the authors, of Tozzi (1992) and of Lejeune et al. (1995), whereas in the tests of Diez-Cascon et al. (1991), a quasi-uniform flow seem to have been reached; and (4) for very high H_d/y_c, the mean air concentration approaches the equilibrium value estimated for a conventional chute of identical slope.

Considering the nature of the experimental data, the techniques used to estimate C (with the exception of that of the authors), and also noting that the effect of the roughness was not accurately taken into account (which is particularly important for low H_d/y_c), the simplified formula included in Fig. 18, based upon all experimental data, is only intended to provide a qualitative indication of the rate of growth of C down the stepped chute.

VELOCITY DISTRIBUTION

In their paper, the authors indicate that, in general, the velocity of the air-water mixture increased continuously with the normal distance from the bed of the stepped spillway, reaching a maximum value at a distance of y_{um}. It was also pointed out that y_{um} was always greater than the transitional depth y_t and lower than $y_{0.9}$. On the other hand, other researchers (Tozzi 1992; Boes and Hager 1998) obtained velocity profiles in fully developed skimming flow which indicate that the velocity increases continuously up to ''free surface'' (Tozzi 1992, pp. 67–69) or to the depth defined as $y_{0.9}$ (Boes and Hager 1998). Tozzi (1992) measured velocities with a conventional Pitot tube and also by using a velocity instrument similar to that developed by Straub et al. (1954), which measured the time for a small slug of salt solution to travel the known distance between two pairs of electrodes aligned with the flow. The velocity measurements with this latter instrumentation compared well with those obtained with the Pitot tube, for $y < y_{um+}$ (where y_{um+} refers to Tozzi's maximum velocity obtained with the conventional Pitot tube). A camera video was also used by Tozzi to estimate the velocity of some tracing targets carried by the flow near the ''free-surface,'' and the results were found to agree with the data obtained with the above-mentioned velocity instrument (Tozzi 1992, p. 67). Recently, Boes and Hager (1998) used a fiber-optical probe to measure the velocity of the air-water interface (which equals the water velocity for $y < y_{0.9}$, assuming no slip between air and water phases), and it was found that all the data collapsed on a power law curve similar to that observed in conventional chutes (e.g., by Cain and Wood 1981 and by Chanson 1989, 1993).

In the discusser's view, the discrepancies between the authors' velocity profiles and those of Tozzi (1992) and Boes and Hager (1998), for $y_{um} < y < y_{0.9}$, might be a result of the application of (3) for high values of C (e.g., $C > 0.7$).

Researchers such as Viparelli (1953), Lai (1971), and more recently Frizell et al. (1994) used a Pitot/Prandtl tube (along with a mechanical sampler or an electrical probe to measure the local air concentration) to estimate the local water velocity in self-aerated flow. The water (for mixture) velocity can be estimated by (Wood 1983):

$$u = \sqrt{\frac{2\Delta p}{\rho_w(1 - \lambda C)}} \tag{29}$$

where λ is a tapping coefficient that accounts for the nonhomogeneous behavior of the air-water flow approaching the stagnation point of the Pitot tube. In Fig. 19, the tapping coefficient obtained experimentally by Lai (in Cain 1978) and estimated by the discusser from the data of Frizell et al. (1994), is expressed as a function of the mean air concentration. It should be noted that for the data of Frizell et al. (1994), λ is largely greater than 1 because a backflushing flow rate of 3.79 l/h in air was chosen in their laboratory testing. The relative differences by applying (3) and (29) are represented in Fig. 20. Fig. 20 shows that even though λ might always be relatively close to unity (as in Lai's data), the application of (3) (i.e., considering $\lambda = 1$) underestimates notably the velocity for $C > 0.6$ to 0.7. In Fig. 3(b) ($l/h = 0.6$, $h = 125$ mm, $y_c/h = 1.2$), the point where the velocity is maximum corresponds approximately to $y = 70$ mm. According to Fig. 3(a), $C \approx 60\%$ for $y = 70$ mm. Note that the legend of Fig. 3(a) indicates that $y_c/h = 1.0$, which does not appear to be in agreement with the results presented in Fig. 4(b) and (c). From Fig. 3(a), $y_{0.9} \approx 100$ mm and $y_t > 60$ mm, which seem to correspond to $Q = 61.55$ l/s, i.e., $y_c/h = 1.3$ [Figs. 4(b and c) and Table 1]. If this is the case, then for $y = 70$ mm it is likely that C won't be largely different from 60%, being consistent with the idea that (3) should become inexact for $C > 0.6$ to 0.7.

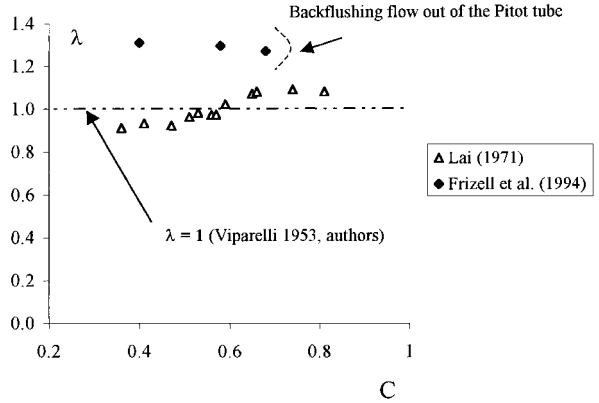

FIG. 19. Effect of Local Air Concentration on Tapping Coefficient of Pitot Tube (after Lai 1971)

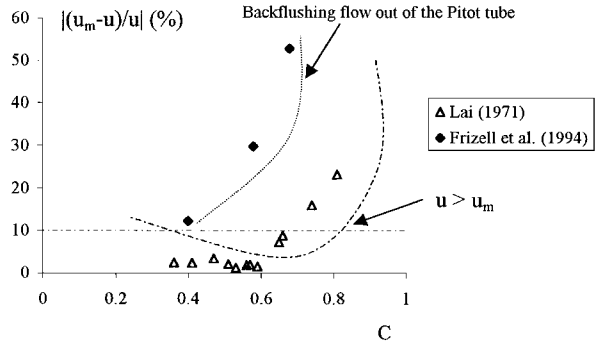

FIG. 20. Relative Differences between Velocity Estimated by (3) and Measured Water Velocity (u)

It is also important to mention that the structure of the flow in the laboratory testing is not expected to be similar to that occurring in the self-aerated flow for high values of the local air concentration. In actual fact, it is not physically possible to obtain homogeneous air-water mixtures for very high air concentrations (i.e., for C greater than about 75%), as mentioned in Falvey (1980) and also experienced by Frizell and others in their calibration tests. In addition, only part of the total air is entrained in the skimming flow for high values of C, the remaining being moved between the highly irregular wavy surface. It is believed that the inexactness of (29) might also be due to the high frequency of the free-surface waves when compared to the time response of the Pitot tube, and possibly to the misalignment between the flow direction and the pseudo-bottom, for $y > y_t$.

Considering the physical nature of the transitional depth y_t, the observations of the authors that y_{um} was always greater y_t seem to be in conformity with the discusser's view [e.g., from Fig. 3(a), $y_t \approx 60\%$). The author's conclusion that the velocity distribution is well described by the Karman-Prandtl equation

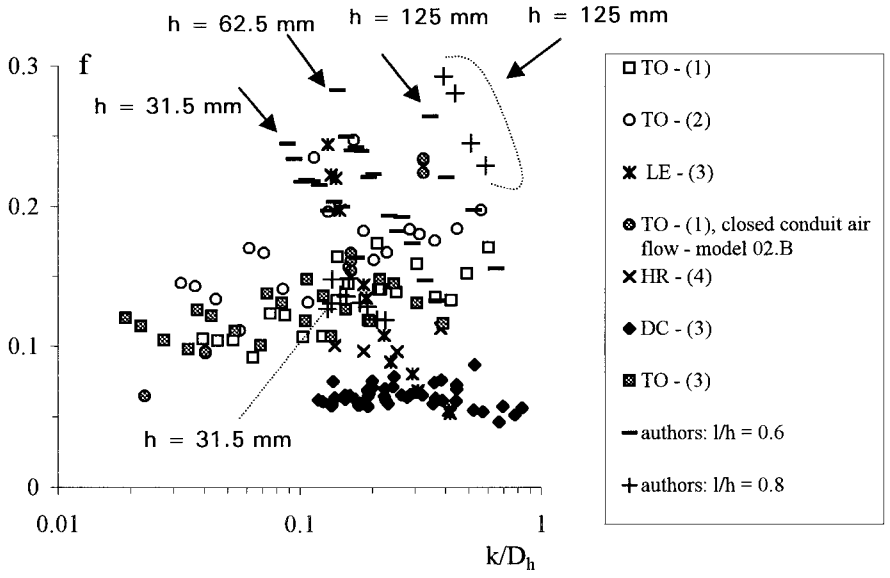

Notes:
HR - Houston and Richardson (1988); TO - Tozzi (1992); DC - Diez-Cascon et al. (1991); Lejeune, Lejeune and Lacroix (1994). Recalculated f by using: (1) characteristic flow depth; (2) equivalent clear water depth; (3) - equivalent clear water depth at the toe, non-intrusive for Diez-cascon et al. (1991) and Tozzi (1992) or intrusive for Lejeune, Lejeune and lacroix (1994); (4) velocity at the toe (Pitot tube or tracing targets with a video or high speed movie camera).

FIG. 21. Friction Factor in Skimming Flow over Steep Step Spillways (after Matos and Quintela 1995a)

only for $y < y_{um}$ is also judged to support of the above reasoning.

FLOW RESISTANCE AND ENERGY DISSIPATION

The authors have compared the skin friction coefficient c_f obtained from investigations on sand roughness pipes (by Nikuradse), pool and weir fishways (by Sikora), and in stepped spillway model chutes (By Sorensen 1985; Diez-Cascon et al. 1991; Bayat 1991; Bindo et al. 1993; Christodoulou 1993; Tozzi 1994; and by the authors themselves) and found that the process of averaging c_f (excluding the data of Bayat 1991 and Bindo et al. 1993) brought some order to the data sets. The process of averaging c_f for a range of flow rates seems acceptable for the uniform flow regime in fully rough turbulent flows, because c_f is not greatly dependent on the water discharge. However, the following questions may be raised: Have uniform flow conditions been attained in all of the stepped spillway model chute experiments? What is the expected effect of air entrainment on c_f, for identical k/Y?

Attempts have been made recently to explain the scatter of the friction factor f in skimming flow over stepped spillways (e.g., Matos and Quintela 1995a; Matos 1997). In those studies, f has been estimated as $f = 8g \sin\theta\, d^3/q^2$, where d is the equivalent clear water depth, as adopted by Wood (1983, 1991) and Chanson (1994). The importance of using identical criterion for the definition of the depth d, when comparing different sets of data, was found to be very important (Matos 1997).

In Fig. 21, the friction factor obtained from the authors' data (Table 1) has been included, and it can be observed that f is of the same order of magnitude as that based on Tozzi (1992). It can also be noted that the data of the authors follow the same trend as that exhibited in other studies (Tozzi 1992; Lejeune et al. 1994), i.e., for constant step height, f seems to decrease with increasing k/D_h. This trend contrasts with that commonly reported in classical clear water flow experiments (e.g., by Nikuradse). On the other hand, the f values recalculated from Diez-Cascon et al. (1991) by the application of the nonintrusive method (as described in Matos and Quintela 1995a) were found to be practically constant, but significantly lower than those obtained from the other studies. If it is agreed that large quantities of entrained air significantly reduces the friction factor in self-aerated flow (e.g., Wood 1983; Chanson 1993), then the examination of Fig. 18 might explain the above-mentioned results. In fact, uniform fully aerated flow conditions seem to have been attained only in the experimental tests of Diez-Cascon et al. (1991).

The authors' results presented in Fig. 9 are also important because they confirm that the rate of energy dissipation is significantly lower than that usually predicted on the basis of bulked flow depth measurements, as suggested in previous studies (e.g., Matos and Quintela 1995a–c).

APPENDIX. REFERENCES

Afshar, N. R., Asawa, G. L., and Ranga Raju, K. G. (1994). "Air concentration distribution in self-aerated flow." *J. Hydr. Res.*, Delft, The Netherlands, 32(4), 623–631.

Boes, R. M., and Hager, W. H. (1998). "Fiber-optical experimentation in two-phase cascade flow." *Proc., Int. RCC Dams Seminar*, K. Hansen, ed., EUA, Denver.

Cain, P. (1978). "Measurements within self-aerated flow on a large spillway." *Res. Rep. No. 78-18*, University of Canterbury, Christchurch, New Zealand.

Cain, P., and Wood, I. R. (1981). "Measurements of self-aerated flow on a spillway." *J. Hydr. Div.*, ASCE, 107(11), 1425–1444.

Chanson, H. (1989). "Flow downstream of an aerator-aerator spacing." *J. Hydr. Res.*, Delft, The Netherlands, 27(4), 519–536.

Chanson, H. (1993). "Self-aerated flows on chutes and spillways." *J. Hydr. Engrg.*, ASCE, 119(2), 220–243.

Falvey, H. T. (1980). "Air-water flow in hydraulic structures." *USBR Engrg. Monograph*, 41, Denver.

Frizell, K. H., Ehler, D. G., and Mefford, B. W. (1994). "Developing air concentration and velocity probes for measuring in highly-aerated, high-velocity flow." *Proc., Symp. on Fundamentals and Advancements in Hydr. Measurements and Experimentation*, C. A. Pugh, ed., ASCE, New York, 268–277.

Hager, W. H. (1991). "Uniform aerated chute flow." *J. Hydr. Engrg.*, ASCE, 117(4), 528–533.

Houston, K. L., and Richardson, A. T. (1988). "Energy dissipation characteristics of a stepped spillway for an RCC dam." *Proc., Int. Symp. on Hydr. for High Dams*, IAHR, Delft, The Netherlands, 91–98.

Lai, K. K. (1971). ''Studies of air entrainment on steep open channels.'' MSc thesis, University of New South Wales, Sydney, Australia.
Lejeune, A., Lejeune, M., and Lacroix, F. (1994). ''Study of skimming flow over stepped spillways.'' *Proc., Int. Conf. on Modelling, Testing and Monitoring for Hydro Powerplants*, HP&D, Budapest, Hungary, July, 285–294.
Matos, J. (1995). ''Discussion of 'Air concentration distribution in self-aerated flow.' '' *J. Hydr. Res.*, Delft, The Netherlands, 32(4), 589–592.
Matos, J. (1997). ''Discussion of 'Model study of a roller compacted concrete stepped spillway.' '' *J. Hydr. Engrg.*, ASCE, 123(10), 933–936.
Matos, J., and Frizell, K. H. (1997). ''Air concentration measurements in highly turbulent aerated flow.'' *Proc., 28th IAHR Congr.*, Theme D, Vol. 1, Sam S. Y. Wang and Torkild Carstens, eds., San Francisco, 149–154.
Matos, J., and Quintela, A. (1995a). ''Flow resistance and energy dissipation in skimming flow over stepped spillways.'' *Proc., 1st Int. Conf. on Water Resour. Engrg.*, ASCE, New York, Vol. 2, 1121–1126.
Matos, J., and Quintela, A. (1995b). ''Discussion of 'Comparison of energy dissipation between nappe and skimming flow regimes on stepped chutes.' '' *J. Hydr. Res.*, Delft, The Netherlands, 33(1), 135–139.
Matos, J., and Quintela, A. (1995c). ''Energy dissipation in skimming flow over stepped spillways. A comparative analysis.'' *Proc., 26th IAHR Congr.*, London, Vol. 1, 370–372.
Ruff, J. F., and Frizell, K. H. (1994). ''Air concentration measurement in highly turbulent flow on a steeply-sloping chute.'' *Proc., Hydr. Engrg. Conf.*, George V. Cotroneo and Ralph R. Rumer, eds., ASCE, New York, Vol. 2, 999–1003.
Tozzi, M. J. (1992). ''Caracterização/comportamento de escoamentos em vertedouros com paramento em degraus'' (''Hydraulics of stepped spillways''). PhD thesis, University of São Paulo, Brazil (in Portuguese).
Viparelli, M. (1953). ''Flow in a flume with 1:1 slope.'' *Proc., Minnesota Int. Hydr. Con.*, IAHR/ASCE, Minneapolis, Minnesota, 415–423.
Wood, I. R. (1983). ''Uniform flow region of self-aerated flow.'' *J. Hydr. Div.*, ASCE, 109(3), 447–461.
Wood, I. R. (1984). ''Air entrainment in high speed flows.'' *Proc., Int. Symp. on Scale Effects in Modelling Hydr. Struct.*, IAHR, Esslingen am Neckar, Set., Germany. H. Kobus, ed., Paper 4.1, 4.1.-1–4.1.-7.
Wood, I. R. (1991). ''Free-surface air entrainment on spillways.'' *Air entrainment in free surface flows*, Ian R. Wood, ed., IAHR, Hydraulic Structures Design Manual No. 4, Hydraulic Design Considerations, Balkema, Rotterdam, The Netherlands, 55–84.
Wood, I. R. (1995). ''Discussion of 'Air concentration distribution in self-aerated flow.' '' *J. Hydr. Res.*, Delft, The Netherlands, 32(4), 582–585.

Discussion by I. Ohtsu,[6] Y. Yasuda,[7] and M. Takahasi[8]

The discussers have investigated the friction factor of stepped flows under a wide range of slopes θ, relative step heights h/y_c, and relative dam heights H_{dam}/y_c (H_{dam} = height of dam) (Yasuda and Ohtsu 1999). Recently the air concentration of stepped flows has been studied, and the distribution of air concentration at each section has been obtained. Further, the equilibrium condition for stepped flows has been clarified by considering the jump formed immediately below the stepped spillway.

The discussers would like to comment on the friction factor and the air concentration of skimming flows.

EQUILIBRIUM CONDITION OF SKIMMING FLOWS

For a given channel slope θ, step height h, and discharge q (or critical depth y_c), as the downward distance along a stepped channel becomes long, a quasi-uniform flow is reached at a certain section of the stepped channel. In order to determine the equilibrium condition, the sequent depth of a jump immediately below the stepped spillway has been utilized (Yasuda and Ohtsu 1999). The toe location of the jump is defined as the section at which the bed pressure is at its maximum, due to the curvature of streamline. For the quasi-uniform flow, the subcritical depth of the jump h_2/y_c becomes a constant value under given channel slope θ and relative step height h/y_c. The relative distance below the crest H_e/y_c (Fig. 22) required to form the quasi-uniform flow for θ = 55° can be predicted by the following equation:

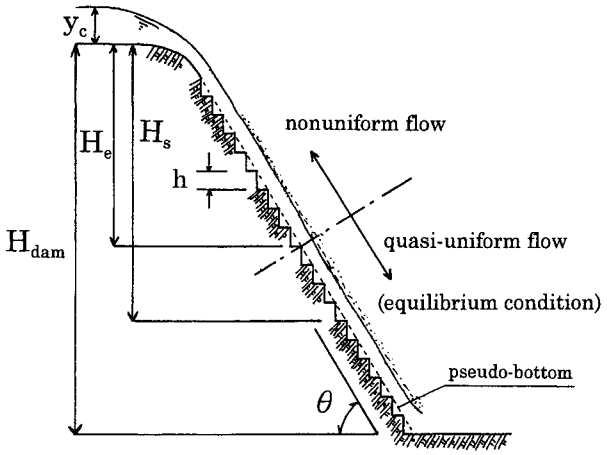

FIG. 22. Equilibrium Condition in Skimming Flows

$$H_e/y_c = 28 + 30 \exp(-10h/y_c),$$

$$\text{for skimming flow } (0 < h/y_c \leqq 1.25 \text{ and } \theta = 55°) \qquad (30)$$

FRICTION FACTOR OF SKIMMING FLOWS

If the friction factor of skimming flows under an equilibrium condition is defined as (31), the friction factor **f** depends on the channel slope θ and the relative step height h cos θ/d_O, as shown in Fig. 23.

$$\mathbf{f} = 4C_{fw} = \frac{4\tau_O}{\frac{1}{2}\rho_w V_O^2} = \frac{8gd_O \sin\theta}{V_O^2} = 8\left(\frac{d_O}{y_C}\right)^3 \sin\theta \qquad (31)$$

where ρ_w = mass density of water; V_O = average velocity of clear water ($=q_W/d_O$); q_W = water discharge per unit width; and d_O = quasi-uniform flow depth on the stepped channel, which is calculated by using (32) and (33):

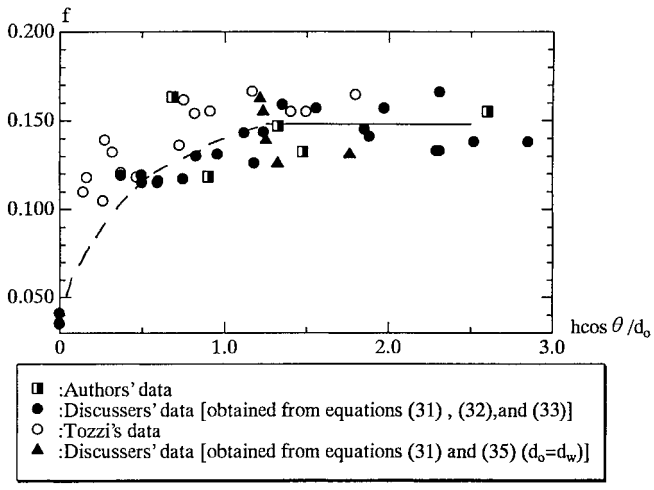

FIG. 23. Friction of Skimming Flows under Equilibrium Condition

[6]Prof., Dept. of Civ. Engrg., Nihon Univ., Coll. of Sci. and Tech., Kanda Surugadai, 1-8 Chiyoda-ku, Tokyo 101-8308, Japan.
[7]Asst. Prof., Dept. of Civ. Engrg., Nihon Univ., Coll. of Sci. and Tech., Tokyo, Japan.
[8]Res. Assoc., Dept. of Civ. Engrg., Nihon Univ., Coll. of Sci. and Tech., Tokyo, Japan.

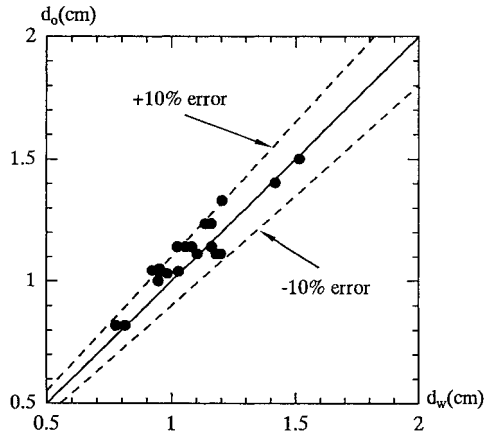

FIG. 24. Comparison of Supercritical Depth in Skimming Flows between Direct and Indirect Measurements

$$\frac{w_w}{g} q_w(v_2 - v_1) = \frac{1}{2} w_w h_p h_1 - \frac{1}{2} w_w h_2^2 \tag{32}$$

$$H_1 = \frac{v_1^2}{2g} + \lambda h_1 = \frac{v_O^2}{2g} + d_O \cos\theta \tag{33}$$

Here, v_1 and h_1 = averaged velocity and supercritical depth at the toe of the jump; v_2 and h_2 = averaged velocity and subcritical depth at the end of the jump; h_p = pressure head at the channel bottom; and λ = pressure distribution coefficient:

$$\lambda = 1 + \frac{1}{Pwgqwh_1} \int_0^{h_1} u\Delta p \, dy \tag{34}$$

Further, u is the velocity at the toe of the jump and is experimentally approximated as $u = U(y/h_1)^{1/8}$; and Δp is the deviation from the hydrostatic pressure [$p_s = w(h_1 - y)$] and given as $\Delta p = w(h_p - h_1)\,(h_1 - y)/h_1$; h_p has been measured experimentally.

As a nonintrusive method for estimating the supercritical depth d_O, the momentum (32) has been applied to the hydraulic jump that is formed immediately below the stepped channel end (Yasuda and Ohtsu 1999). Also, the application of (33) indicates that the total head of the quasi-uniform flow in the stepped channel [$v_O^2/(2g) + d_O \cos\theta$] coincides with that at the toe of the jump [$v_1^2/(2g) + \lambda h_1$] under given tan θ, h/y_C, and H_S/y_C.

It has been verified experimentally that the supercritical depth d_O calculated by using (32) and (33) coincides with the clear water depth d_W obtained by the following relation, within $\pm$10% error (Fig. 24):

$$d_W = \int_0^{y_{0.9}} (1 - C)\, dy = (1 - \bar{C}) y_{0.9} \tag{35}$$

Also, it has been confirmed from the discussers' experiments that the specific energy of the stepped channel flow [$(q_w/d_W)^2/2g + d_W \cos\theta$] coincides with the total head at the toe of the jump under given tan θ and h/y_C.

In Fig. 23, the authors' data and Tozzi's data have been plotted under an equilibrium condition in which the value of H_S/y_C (H_S = vertical distance from the top of crest to the test section) is larger than the value of H_e/y_C calculated by (30). Here, the value of H_{dam} in the authors' paper is taken as H_S = 2.5 m. As shown in this figure, a comparison of the authors' and Tozzi's data with the discussers' data shows the same tendency.

CHARACTERISTICS OF AIR CONCENTRATION FOR SKIMMING FLOWS

Fig. 25 shows the distribution of air concentration in a quasi-uniform flow for θ = 55°. In this figure, y is the normal distance above the pseudo-bottom. As shown in Fig. 25, the distribution at the edge section (a-a) differs from that at the corner section (b-b). In particular, the air concentration near the pseudo-bottom at the corner section is larger than that at the edge section, because a recirculation vortex with large quantities of air-bubble is formed below the pseudo-bottom.

In addition, the authors' distribution of air concentration [Fig. 3(a)] is the same as the discussers' distribution at the edge section for θ = 55°, h/y_C = 0.77, and H_S/y_C = 14-15 (nonequilibrium condition) (Fig. 26).

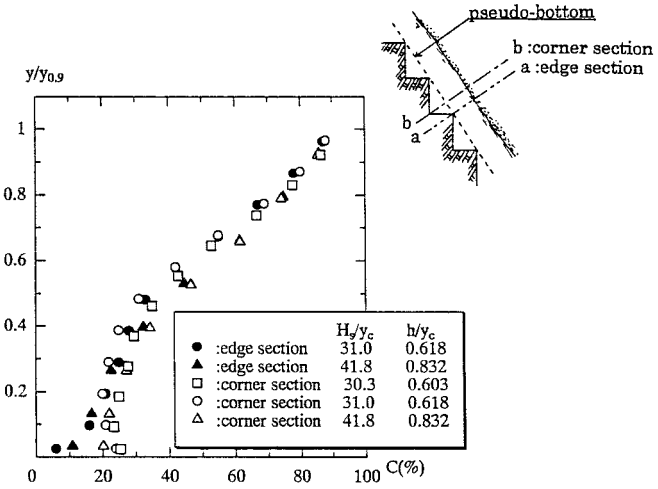

FIG. 25. Distribution of Air Concentration for Skimming Flows under Equilibrium Condition (θ = 55°)

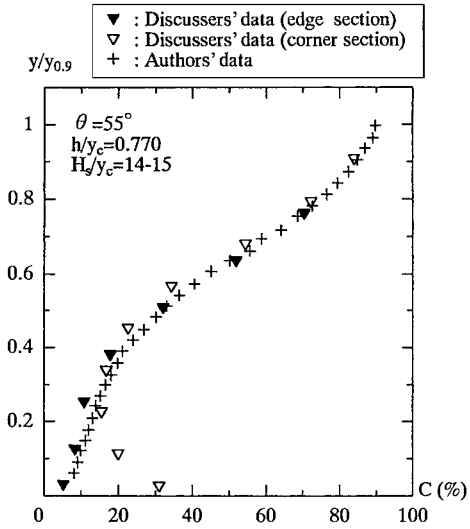

FIG. 26. Distribution of Air Concentration in Skimming Flow

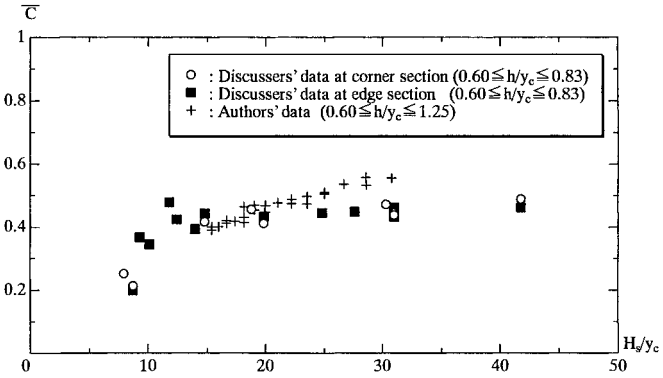

FIG. 27. Average Value of Air Concentration at Each Section in Skimming Flows (θ = 55°)

Fig. 27 shows an example of the relationship between the average value of air concentration C and the relative distance below the crest H_S/y_C under given channel slope θ and the relative step height h/y_C. As shown by this figure, the average air concentration C changes with H_S/y_C for $H_S/y_C < 15$. For $H_S/y_C \geqq 15$, the change of C with H_S/y_c is very small and the value of C is almost constant. The authors' data (data for $0.6 \leqq h/y_C \leqq 1.25$) show the same trend.

APPENDIX. REFERENCES

Ohtsu, I., and Yasuda, Y. (1997). "Characteristics of flow conditions on stepped channels." *Proc., Theme D, 27th Congr. of IAHR*, San Francisco, Aug., 583–588.

Yasuda, Y., and Ohtsu, I. (1999). "Flow resistance of skimming flow in stepped channels." *Proc., 28th Congr. of IAHR, Theme B, Hydr. Struct., Spillways and Chute Struct.*, B14, Graz, Austria, Europe.

Discussion by Sandip P. Tatewar,[9] Ramesh N. Ingle,[10] and Prakash D. Porey[11]

The authors are to be commended for providing experimental data on a relatively large model of a stepped spillway for skimming flow regime. Most of the earlier investigations are on small models where air entrainment is negligible. The measurement of flow depth on a large model of stepped spillway is difficult because of the air entrainment and large turbulence that generally occurs. Hence, it is difficult to determine the free surface of flow, as there is large variation in its position. Therefore, flow depth and velocity measured at the toe of the spillway model do not give a correct assessment of the energy dissipation. The authors found that the depth at which the air concentration is equal to 90% can be considered as the depth of aerated flow on the stepped spillway. Further, the authors suggested that this flow depth can be used for computation of the skin friction coefficient and relative energy loss over the stepped spillway. On many occasions, computation of flow depth $y_{0.9}$, from the properties of flow and the characteristic dimensions of the stepped spillway, would be required. Flow depth $y_{0.9}$ can be computed by using the authors' (15) and (16). However, these equations are implicit in nature and not convenient for computation of $y_{0.9}$. Therefore, explicit relation based on the authors' data could be useful, and such a relation is developed by the discussers. Flow depth $y_{0.9}$ can be expressed as

$$y_{0.9} = f(q, h, l, g) \tag{36}$$

In dimensionless form (36) can be written as

$$\frac{y_{0.9}}{h} = f\left(\frac{q^2}{gh^3}, \frac{h}{l}\right) \tag{37}$$

Using the authors' data given in Table 1, following equation for computation of $y_{0.9}$ is obtained by regression analysis:

$$\log\left(\frac{y_{0.9}}{h}\right) = 0.3011 \log\left(\frac{q^2}{gh^3}\right) + 0.01696 \log\left(\frac{h}{l}\right) - 0.2053 \tag{38}$$

with coefficient of determination $R^2 = 0.99$.

Using (38) for known values of parameters, the flow depth $y_{0.9}$ can be computed. Diez-Cascon et al. (1991) suggested a method for computation of flow depth at the toe of spillway after considering the effect of air entrainment. Figs. 28 and 29 show the comparison between experimental and calculated values.

Based on their experimental observations, the authors state that the relative energy loss for skimming flow regime varies in the range of 48–63% (Fig. 9). Further, referring to Chamani and Rajaratnam (1994), they mention that the relative energy loss for jet flow regime is much higher. However, it should be noted that the slope of downstream face of spillway in these two cases is different. For the experimental observations for skimming flow, the downstream slope is much steeper than the observations on the model used for jet flow. The relative energy loss depends on the downstream slope of spillway and is higher for mild slopes. This is also reported by Israngkura and Chinnarasri (1994). Further, Chanson (1994) stated that the relative energy loss is higher for skimming flow regime for long chutes, as compared with jet flow regime. Commentary on the comparison of relative energy loss in skimming flow regime and jet flow regime for the same downstream slopes of spillway is desired from the authors.

APPENDIX. REFERENCES

Chanson, H. (1994). "Comparison of energy dissipation between nappe and skimming flow regimes on stepped chutes." *J. Hydr. Res.*, Delft, The Netherlands, 32(2), 213–218.

[9]Asst. Prof., Dept. of Civ. Engrg., Government Coll. of Engineering, Amaravati–444 604, India.

[10]Prin., Yashvantrao Chavan Coll. of Engineering, Wanadongari, Nagpur, India.

[11]Prof., Dept. of Civ. Engrg., Visvesvaraya Regional Coll. of Engineering, Nagpur, India.

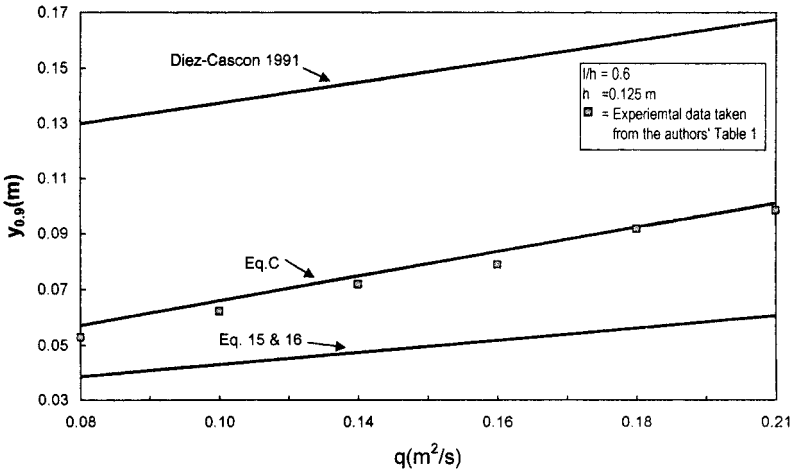

FIG. 28. Comparison of Experimental and Calculated Values of $y_{0.9}$ for $l/h = 0.6$ and $h = 0.125$ m

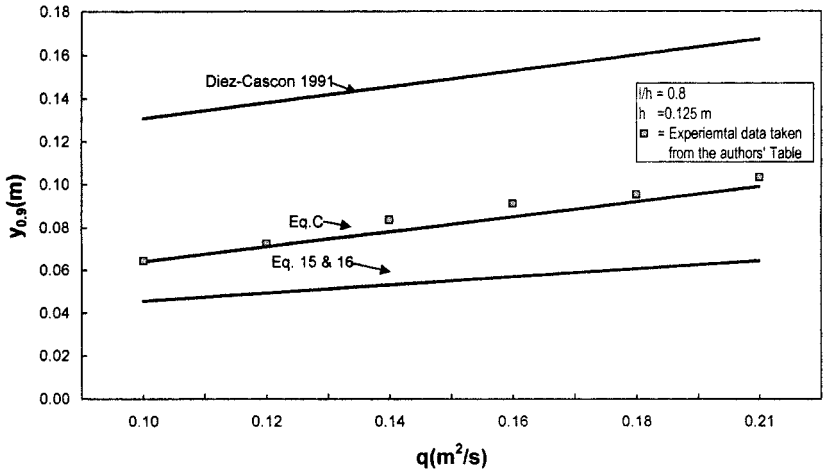

FIG. 29. Comparison of Experimental and Calculated Values of $y_{0.9}$ for $l/h = 0.8$ and $h = 0.125$ m

Israngkura, V., and Chinnarasri, C. (1994). "Flow depth and energy loss through stepped chutes." *Proc., 9th IAHR Congr. of the Asian and Pac. Div.*, International Association of Hydraulic Research, Delft, The Netherlands, Vol. 2, 156–163.

Closure by M. R. Chamani[12] and N. Rajaratnam[13]

The authors are thankful to all the writers for their valuable discussions. They are thankful to Matos for his extensive comments about air concentration profiles and the use of the Prandtl tube for velocity measurement in aerated flows; Tatewar, Ingle, and Porey for their simple equation for calculating the depth of aerated flow; Boes for his comments on the velocity measurement and computation of the skin friction coefficient and relative energy loss; Chanson for his comments on the structure of aerated flows; and Ohtsu, Yasuda, and Takahashi for their data and interesting comparison with the results of the authors. In general, it should be noted that all measurements were carried out at the step-tip sections in the developed region of the air-water mixture, where a condition of equilibrium was attained and the flow characteristics (velocity, air concentration profiles) became approximately invariant. To locate the point where developed flow region starts, air concentrations at different step-tips along the spillway length were measured. When the difference of the air concentration profiles of two consecutive step-tips was less than about 1%, the second step-tip was assumed to be the starting point of the fully developed region. More details about the measurements are available in the thesis of Chamani (1997).

VELOCITY PROFILES

The Prandtl tube has been used before for the measurement of velocity in air-water flows by earlier investigators like Viparelli (1953) and Tozzi (1994). Based on comparison with measurements with high-speed photography and the comments of the several discussers of this paper, it is believed that the measurements are reasonably accurate in the lower region, whereas in the upper region where the air concentration is large, the measurements remain to be checked with observations to be made with more reliable instruments. Perhaps the fiber-optic probe used by Boes would provide these measurements. From the results of a study on very high velocity water jets in air (Rajaratnam et al. 1994; Rajaratnam and Albers 1998), it appears that in the upper regions the velocity of the flow might decrease because of the drag that would be faced by the water drops traveling through the air stream. Velocity measurement in aerated flow is indeed difficult. The velocity profiles were plotted on a semilog sheet with the origin located such that the profiles were linear in the lower region, and the characteristic coefficient in the Karman-Prandtl equation was found which was then used to calculate the equivalent roughness.

AIR CONCENTRATION

The electrical method of measuring air concentration in an air-water mixture relies on the measurement of electrical conductivity of the air-water mixture. A comparison of the electrical probe and the mechanical sampler by Lamb and Killen (1950) showed a very good agreement. In their experiments, the electrical probe was found to measure the air concentration as high as 90% with good accuracy.

The writers used the Straub and Anderson (1958) model mainly because it appeared to be simple and adequate, but comparison with the ideas of Wood and Chanson (demonstrated by Chanson) appears to be interesting. As pointed out by Chanson and Matos, the caption of the writers' Fig. 3(b) should read $y_c/h = 1.3$, not 1.2.

SKIN FRICTION COEFFICIENT

It should be noted that in (15), the skin friction coefficient is determined from each data point, while in (16), the average skin friction coefficient is calculated based on each data set for a specified slope and step height. Therefore, the coefficient, c_f is not the same in (15) and (16) and these equations cannot be combined to determine $y_{0.9}$. It is interesting to see that our results for the skin friction coefficient agree well with those of Ohtsu et al.

ENERGY DISSIPATION

It is interesting to observe the comparison of our results with those of Boes on energy dissipation and skin friction coefficient. Regarding the energy dissipation calculation, it is necessary to mention in (18) for E_b,

[12]Asst. Prof., Isfahan Univ. of Tech., Isfahan, Iran 84154.
[13]Prof., Dept. of Civ. and Envir. Engrg., Univ. of Alberta, Edmonton, AB, Canada T6G 2G7.

$$\rho_m(y) = \rho_w[1 - C(y)] \text{ and } \alpha = \frac{1}{V_m^2} \frac{\int_0^{y_s} \rho_m(y)[u_m(y)]^3 \, dy}{\int_0^{y_s} \rho_m(y) u_m(y) \, dy}$$

where α = kinetic energy correction factor for the aerated flow and V_m = average air-water mixture velocity over the entire section. The elevation of water surface, y_s, was chosen as that value of y where the air concentration is equal to 90% ($y_{0.9}$).

APPENDIX. REFERENCES

Rajaratnam, N., Rizvi, S. A. H., Steffler, P., and Smy, P. (1994). ''An experimental study of very high velocity circular water jets in air.'' *J. Hydr. Res.*, Delft, The Netherlands, 32, 461–470.

Rajaratnam, N., and Albers, C. (1998). ''Water distribution in very high velocity water jets in air.'' *J. Hydr. Engrg.*, ASCE, 124(6), 647–650.

Viparelli, M. (1953). ''The flow in flume with 1:1 slope.'' *Proc., Minnesota Int. Hydr. Con.*, Minneapolis, Minn., 415–423.